



HAL
open science

Various double component mode synthesis and sub-structuring methods for dynamic mixed FEM

Pierre Garambois, Sébastien Besset, Louis Jézéquel

► **To cite this version:**

Pierre Garambois, Sébastien Besset, Louis Jézéquel. Various double component mode synthesis and sub-structuring methods for dynamic mixed FEM. *European Journal of Mechanics - A/Solids*, 2015, 53, pp.196-219. 10.1016/j.euromechsol.2015.04.005 . hal-01266856

HAL Id: hal-01266856

<https://hal.science/hal-01266856>

Submitted on 7 Feb 2016

HAL is a multi-disciplinary open access archive for the deposit and dissemination of scientific research documents, whether they are published or not. The documents may come from teaching and research institutions in France or abroad, or from public or private research centers.

L'archive ouverte pluridisciplinaire **HAL**, est destinée au dépôt et à la diffusion de documents scientifiques de niveau recherche, publiés ou non, émanant des établissements d'enseignement et de recherche français ou étrangers, des laboratoires publics ou privés.

Various double component mode synthesis and sub-structuring methods for dynamic mixed FEM

Pierre Garambois^{a,b}, Sebastien Besset^{a,c}, Louis Jezequel^{a,d}

^a*Laboratoire de Tribologie et Dynamique des Systèmes, UMR CNRS 5513
Ecole Centrale de Lyon, 36 avenue Guy de Collongue 69134 Ecully Cedex, France*

^b*pierre.garambois@ec-lyon.fr*

^c*sebastien.besset@ec-lyon.fr*

^d*louis.jezequel@ec-lyon.fr*

Abstract

This paper presents various sub-structuring and component mode synthesis (CMS) reduction methods for dynamic mixed displacement-stress FEM. The idea is to imagine a new way of reducing a mixed FEM, by splitting the reduction of the displacement and the stress parameters and adapting primal existing modal reduction methods to each field of the mixed model. In this way, we can choose, for each sub-structure, different methods to truncate the displacements, the stresses and even the junction between the sub-structures. The results differ according to the combination of the methods used, and can show extremely promising results that significantly decrease the numerical size of the structures and still keep the benefits of the mixed method.

Keywords: Component Mode Synthesis (CMS), Double Modal Synthesis (DMS), reduction methods, mixed finite element, sub-structuring, vibrations, plates.

1. INTRODUCTION

Most of the Finite Element Models (FEMs) used in industry for structural mechanical problems are based on a dynamic primal formulation that exclusively discretizes the displacements. This displacement approach in FEMs was largely developed ([75, 27, 1]). It is fast and efficient, but it necessitates extra calculations and integrations to get the strains and so the stresses, and may presents some computational difficulties when it comes to plate and shell theories representation. Thus, numerical solutions providing stresses as primary results and solving computational problems have always been of a particular interest in mechanical engineering. A force approach based on direct calculation of stress was pioneered in FEMs by Fraeijis de Veubeke [35, 36] and then other investigations by Pian and Tong [55, 68] were made. Another approach, called "mixed formulation" or "Reissner Mixed Variational Theorem" (RMVT), is based on the Hellinger-Reissner (HR) variational functional and defines a new Lagrangian using both displacement and stress fields in the same functional. That formulation was first imagine by Hellinger [41] and Prange [56], and later by Reissner [60, 61, 62] and Arnold [3, 2]. Generalized variational principles are well explained in Washizu's book [71] with various forms and different fields. FEMs implemented with RMVT present two main advantages: a direct access to stress parameters without post-processing, and a better representation of certain two-dimensional theories such as thick plates.

As far as stress access is concerned, researches have been made in order to easily get to the strain and stress fields, starting from a displacement approach. The classical methods used by most of the software in industry is the Gauss Points Method, that approximates an integral of a function with a weighted sum of function values at specified points within the elements. Other stresses and strains

recovery methods were recently developed by Tornabene and Fantuzzi in the field of arbitrarily shaped laminated plates [32, 33, 34, 69]. They implemented a Strong Formulation FEM (SFEM) using the strong formulation of the differential system at the master element level. Such models combined the generality of FEM and the accuracy of Spectral Methods (SM). Their method relies on the use of Generalized Differential Quadrature (GDQ) which approximates the derivatives of a function at any location by a linear summation of all functional values along a mesh line. The key of such a method is the determination of the weighting coefficients, but compared to classical FEM, it allows a little computational effort and accurate numerical results for a smaller number of mesh points. Once the continuity conditions on displacement and stress, and the SFEM itself are built [32], the stress/strain recovery can be made using the GDQ method [33] to approximate derivatives (of both strains/stresses) and the classical Hook's law. That method permits a good representation of both in-plane and out-of-plane stresses/strains, for both static [32, 33, 34, 69] and dynamic [34] analysis. Furthermore, the comparison between approximations techniques such as Radial Basis Function (RBF) and GDQ has been made by these authors [34], as well as stress/strain recovery analysis with Functionally Graded Materials (FGMs) and multi-curved sandwich shell structures using the Carrera Unified Formulation (CUF) and High-order Shear Deformation Theory (HSDT) for the plate theory and continuity [69]. Another way of accessing to strain/stress values within an element is to formulate the initial problem in a "mixed" way, in function of both displacement and stress parameters, using the RMVT.

The use of such a mixed theorem has been mainly popularized in the context of plate and shell structures analysis, when three-dimensional descriptions try to be obtained with two-dimensional models, because it provides some computational advantages regarding such theory. Indeed, structural plates have a multitude of applications in industries and has received the attention of many researchers. The Kirchhoff-Love (KL) thin plate theory, originally developed by Love [49], is simply implementable and takes into consideration bending and twisting moments but doesn't deal with shearing phenomena which appear to be essential in some cases. Thus, the Reissner-Mindlin (RM) theory for thick plates naturally appeared [59, 51]. Nevertheless, thick RM plate may suffer from "shear-locking" problems and their representation can be tricky. In order to avoid computational problems, solutions have been imagined over the years [44, 8, 9, 47, 65, 13, 46, 52, 73] and among them, mixed type methods have shown very successful results [63, 30, 31, 66, 67, 5], and thus justify its wide use in addition to the stress access previously mentioned. Herrmann implemented one of the first mixed plate FEM using this RMVT and taking shear phenomena into consideration [42, 43], quickly followed by other researchers [16, 25]. Over the last forty years, many mixed FEMs have been implemented for different theory such as 3D problems [54], elastic arches problems [40], Timoshenko's beams [66, 67] and of course particularly for plates [66, 67, 31, 30, 63]. Wriggers' book [72] provides a wide range of application for mixed FEM. Stability [6, 14] and convergence [4] depending on the space fields of such elements have also been widely discussed.

Most of the time, mixed finite element are used in the field of plates and especially in the field of laminated multilayered plate structure and piezoelectric multilayered structures because of the increasing use of composites in thick and thin structures in industry. Indeed, the evaluation of normal stress and transverse shear is crucial in composites. It is well-explained by Carrera [18, 19, 17] that compatibility/equilibrium equations lead to discontinuous derivative and that zig-zag form of transverse displacement, interlaminar continuity for the transverse shear and normal stress must be considered (it is called C_z^0 -requirement [17]). Equivalent Single Layer (ESL) models using displacement approach have been imagined to represent multilayered structure. They present the advantage of a number of unknowns independent from the number of layers. Nevertheless, First-order Shear

Deformation Theory FSDT [74] doesn't respect the C_z^0 -requirement, and post-processing of shear stress shows inaccurate results in the case of thick plates [48]. Furthermore, High-order Shear Deformation Theory (HSDT [48]), developed by Cho and Parmerter [26], although including partial C_z^0 -requirement, experiences difficulties with analyzing problems in which out-of-plane stress play an important role. Another model called LayerWise Model (LWMs) considers each layer as a single plate [64, 57] and is logically more expensive than ESL models. It gives acceptable accuracy but does not a priori fulfill interlaminar C_z^0 -requirement in displacement approach. Thus, mixed models using RMVT retain attention in this field as they a priori and completely verify C_z^0 -requirement, and give a good description of transverse stresses. In this way, mixed layerwise theory to calculate in-plane and out-of-plane stresses/strains for thick multilayered orthotropic laminated plates have been implemented by Carrera for static analysis [19, 23, 24], thermo-static stress analysis [20] and well reviewed in [21] for both ESL and LWM theories. FEMs deep development of such theory is also available in [23, 24]. The comparison between the Principle of Virtual Displacements (PVD) used in primal displacement approach and RMVT-based mixed model [19, 21, 23, 24] gives a clear advantage to the mixed formulation, in terms of interlaminar displacement and stress continuity as well as a good description of stresses within the structure.

As far as piezoelectric adaptive plate is concerned, mixed formulation has also proved to be efficient. Although primal models exist [10], and some of them fulfill interlaminar continuity implementation [18], the use of mixed Layerwise theory for piezoelectric adaptive structure has also proved to be of a high interest in static and modal analysis [38, 39], thermodynamic analysis [11]. Carrera and Boscolo's article [22] shows an extension to electro-mechanical piezoelectric plate problems of a previously cited article by Carrera [23, 24] on both primal and mixed FEM for multilayered plate elements using both ESL and LWM theories. This article puts forward another use and interest of mixed model in structural mechanical and FEMs analysis.

In this paper, the mixed FEM we use as an example for the reduction methods, is implemented with thin KL plate elements, which means that the stress parameters are actually generalized stress parameters. Most of the time, the examples of mixed FEM deals with static analysis in the previous examples. It is more rarely used for free vibrations [53], and when it is, it often condenses the problems with condensed (or equivalent) stiffness on the displacement and then make the calculation only with the displacement field. The mixed model reduced in this paper is indeed a dynamic mixed FEM (DM-FEM) as we take into consideration the kinetic energy in the mixed formulation.

Although advantageous for the reasons previously defined, an obvious inconvenience of the mixed formulation that is not condensed on displacements, is the numerical size of the problems, due to the addition of stress fields parameters (generalized stress in our case) to the displacement field parameters of a regular primal method. Many sub-structuring methods exist so as to reduce primal FEM such as "fixed interface mode" method (Craig & Bampton method [29]), "free interface mode" method (Mac Neal method [50]) and "boundary mode" method (see Brizard [15] and Tran [70]). The principle of those methods is to split the structure into a few sub-structures, and to express the behavior of each one taking separately with its own eigenmodes (the type of eigenmodes depending on the method). Some of those methods have also been associated to build up a Double Modal Synthesis (DMS) or Double Component Mode Synthesis (see Jezequel [45]) and Besset [12]) where we both condense the sub-structures and the junction between them with "boundary modes". In the case of a mixed FEM, the obtaining of singular matrix makes it impossible to compute the modes of the structure, and so to use those methods, as originally formulated. In this paper, we adapt those primal methods to build a new reduced basis for each mixed sub-structure. That possibility has

already been discussed in [37] using "fixed interface method" and keeping the boundary as is. In this paper we aim at developing this principle with all the methods previously defined and to introduce a boundary condensation as well, to turn the reduction into a DMS. The main idea is, for each sub-structure, to separate the condensation of each of the two fields, using one of the primal existing methods for the condensation of the displacements and another method (or possibly the same) for the stresses. Thus, we can choose the type of method to apply on each field separately and treat the reductions in a separated way, as well as the boundary condensation. Then we assemble the structures through the displacement parameters. It sounds important to notice that the method we implement here is the same for any displacement-stress mixed FEM using any mechanical theory (plate, beam, 3D, arches...).

First of all, the article talks about the HR mixed variational dynamic formulation and its adaptation to FEMs and the principle of such a model in general. Afterwards, we deal with the presentation of the sub-structuring method, the various double component mode synthesis methods we aim at using in it and of course the application of those methods to a mixed FEM by splitting the reduction of each field separately. In the last part, we present a little mixed FEM example using thin Kirchhoff-Love plate theory, apply all the methods for a simple case, and show the results depending the chosen methods and the chosen truncations.

2. MIXED VARIATIONAL FORMULATION AND MIXED FINITE ELEMENT MODEL BASED ON THICK AND THIN PLATE THEORIES

In this section, we use Einstein summation convention to manipulate physical equations with coordinates. The Cartesian coordinates system leads us to a subscript i that corresponds to x, y, z .

2.1. The mixed finite element formulation

Our displacement-stress DM-FEM is based on the HR mixed functional [41, 60, 61, 62] expressed for dynamics problems, which may correspond to the regular Lagrangian used in dynamics, but computed with mixed component. Basically, it means that the potential energy and the kinetic energy are expressed with both displacement and stress fields whenever possible. In this way, the HR dynamic functional can be given by:

$$\Pi_{HRD} = \iiint_V -\sigma_{ij} e_{ij}(\mathbf{u}_i) + \frac{1}{2} \sigma_{ij} \mathbf{S}_{ijkl} \sigma_{kl} + \mathbf{b}_i \mathbf{u}_i + \frac{1}{2} \rho \dot{\mathbf{u}}_i^2 \, dV \quad (1)$$

considering σ_{ij} the stress, \mathbf{u}_i the displacement, $e_{ij}(\mathbf{u}_i)$ the strain function of the displacement \mathbf{u}_i , \mathbf{b}_i the body force, ρ the volumic mass, V the volume, and \mathbf{S}_{ijkl} the elastic compliance matrix.

2.2. Discretization of the fields

The interpolation of the displacements and strains is given by:

$$\mathbf{u}_i = \mathbf{N} \mathbf{U} \quad (2)$$

$$\sigma_{ij} = \mathbf{P} \boldsymbol{\beta} \quad (3)$$

with \mathbf{N} and \mathbf{P} being respectively the matrix of the displacement and stress shape functions, and \mathbf{U} and $\boldsymbol{\beta}$ the displacement and stress parameters. The strain is derived from the displacements as:

$$\mathbf{e}_{ij} = \mathbf{D} \mathbf{u}_i \quad (4)$$

with \mathbf{D} being the displacement-strain gradient operator.

2.3. Mixed finite element formulation

The HR mixed dynamic formulation presented in equation 1 can be discretized through equations 2 and 3, and the matrix development gives:

$$\underbrace{\begin{Bmatrix} \mathbf{M} & \mathbf{0} \\ \mathbf{0} & \mathbf{0} \end{Bmatrix}}_{\mathbf{M}_{mix}} \begin{Bmatrix} \ddot{\mathbf{U}} \\ \ddot{\boldsymbol{\beta}} \end{Bmatrix} + \underbrace{\begin{Bmatrix} \mathbf{0} & \mathbf{G}^T \\ \mathbf{G} & \mathbf{H} \end{Bmatrix}}_{\mathbf{K}_{mix}} \begin{Bmatrix} \mathbf{U} \\ \boldsymbol{\beta} \end{Bmatrix} = \begin{Bmatrix} \mathbf{F} \\ \mathbf{0} \end{Bmatrix} \quad (5)$$

where

$$\mathbf{M} = \iiint_V \mathbf{N}^T \rho \mathbf{N} dV, \quad \mathbf{G} = \iiint_V \mathbf{P}^T \mathbf{D} \mathbf{N} dV, \quad \mathbf{H} = \iiint_V -\mathbf{P}^T \mathbf{S} \mathbf{P} dV \quad (6)$$

and \mathbf{F} is the force vector applied to the mesh nodes.

2.4. Distinctive features of the mixed model and consequences on the calculation

The HR DM-FEM formulation presents a distinctive feature compared to most of the dynamic primal models because of the empty part of the mass matrix in the stress field. Some methods presented in literature [53] consist in using the second line of the matrix system as a relation between displacement and stress, and thus build "equivalent mass and stiffness matrix" \mathbf{M}_{eq} and \mathbf{K}_{eq} condensed on displacements. It is a simpler way of solving an elastic dynamic mechanical mixed problem but it only focuses on the displacements as a first result of the computation.

The main idea of our work is to keep the matrix system as is, and make the computation and reduction of the mixed model in its primary form, to get both displacements and stresses as a primary result.

The drawback of this choice is due to the empty part of the mass matrix in the generalized stress field in the 5 form: we cannot diagonalize the equations and use regular modal synthesis methods.

First consequence of this characteristic: it is complicated to get a quick modal analysis with eigenfrequencies and mixed eigenvectors. We choose to build a Frequency Response Function (FRF) on a wide frequency band so as to get both a dynamic mixed response and reach eigenvectors and eigenvalues. The first inconvenience of this method is, of course, the computation speed due to the repetitiveness of a calculation containing an inverse, all the more when the frequency band is wide. The second one is the risk of missing a mode if the frequency spectrum is not discretized enough and if the node we excite/observe is a node of the mode.

Second consequence of this feature: we cannot apply a regular primal modal synthesis method [45] method to reduce the model and increase the computation speed, as we cannot easily compute the mode on a mixed model. The search of the eigenmodes would take too much time. Hence

the idea of a new type of reduction for mixed model, using the primal model. This idea was first imagine in [37], and the goal of this paper is to enlarge those research using different types of primal reduction methods in the mixed adaptation.

It should also be noted that the number of DOFs of one HR mixed element is significantly higher than the same element with the primal formulation as it requires parameters for the stress.

3. MODAL REDUCTIONS ON A MIXED FINITE ELEMENT MODELS

The numerical sizes of the DM-FEM in general are significantly higher than primal models using the same theories and the same amount of elements. The elementary matrix is twice bigger in the case of plate elements using Kirchoff-Love theory. As an example, a rectangular clamped plate composed of about 1000 Kirchoff-Love elements is composed by about 3000 primal DOFs or 12000 mixed DOFs which is 4 times more. It is therefore important to reduce it to increase the computation speed.

The distinctive feature of the mixed model (when it is not condensed on the displacements) is the impossibility to apply a regular modal synthesis method as the mixed matrix cannot be diagonalized. The idea of this part is to reduce the numerical size of the model, by adapting regular sub-structuring methods easily computable for primal FEM, to DM-FEM.

The sub-structuring methods using modal components permit to describe the low frequency phenomenon of a structure by splitting it into sub-structures and using eigenmodes of each sub-structures taking separately. Therefore, "constraint static modes" are used to link them. They permit to offset the truncation of the eigenmodes of each sub-structure, and thus increase the precision of the method.

Many different reduction methods can be used for each sub-structures. So far, they are all based on primal models. There are two main primal modal synthesis method families. The first one is the fixed interface methods described in 1968 for the first time by Craig and Bampton [29, 28]. It is based on eigenmodes of each substructure, assuming that the boundary is held fixed, and constraint static modes (these are substructure response to successive unit boundary displacement). The second family refers to free interface methods and has been released in 1971 for the first time by MacNeal [50]. It is based on eigenmodes of each substructure, assuming that the boundary is free and attachment modes (substructure response to successive unit boundary force). It is important to notice that the regular sub-structuring methods are applied to primal FEM with only one field (displacement), consequently, we present them with the displacement field as a unique field. Then, we explain how to adapt them to mixed model.

The number of boundary modes being equal to the number of boundary DOFs, another reduction was described with Balmes [7] and [15], and leads to a boundary condensation using branch modes. It permits to reduce the boundary to a certain number of "branch modes", depending on the frequency band we want to observe. Thus, the reduction turns into a DMS (see Jezequel [45]).

In the three first sections, we describe respectively the branch modes method featuring the junction between sub-structures, the "fixed mode" method and the "free mode" method. Those three first sections are presented displacement wise because they were imagined for primal analysis. Hence the importance of the fourth section dealing with the projection of the stress parameters on the displacement parameters (actually used for the primal reductions defined before). That section adapt the DMS defined in the three first sections to the stress field, so as to express the reduction of the stress fields using the primal methods. The fifth section deals with the association of the displacement and the stress projection, in order to build a complete mixed reduction (mixed DMS). Indeed, we depict a few different combinations of projections, depending on the one chosen for each field. The table 1 summarizes the different mixed DMS we implemented. It is important to notice that the "Fix-Fix-2" method when not using "branch modes" is the same method as the one described in [37]. In the end, the sixth section deals with the assembly of the sub-structures in function of the method we have chosen.

Table 1: Different types of mixed DMS

Name of reduction	Method for displacement	Method for stress	Branch modes
Fix-Fix-1(/-br)	fixed modes with same parameters		No(/Yes)
Fix-Fix-2(/-br)	fixed modes	fixed modes	No(/Yes)
Fre-Fix-2(/-br)	free modes	fixed modes	No(/Yes)
Fre-Fre-1(/-br)	free modes with same parameters		No(/Yes)
Fre-Fre-2(/-br)	free modes	free modes	No(/Yes)

The structure is supposed to be composed of two sub-structures, which does not restrict the method. A superscript $.^{(s)}$ is added to make the distinction between each substructure s . The subscripts i and j refer to internal and junction DOFs respectively. The subscripts FI refer to "fixed" eigenmodes whereas the subscripts FR refers to "free" eigenmodes. We may also add the subscript (U) and (β) when talking about a mixed formulation to refer to displacement fields and stress field respectively.

3.1. Branch modes

The regular modal synthesis (or CMS) using fixed modes and free modes keep a number of boundary modes equal to the number of junction DOFs. The idea of this part is to condense the boundary through the use of branch modes and to keep only a certain number of boundary modes. The branch modes represent the behavior of the structure condensed on its junction, using "constraint static modes". The "constraint static modes" of the global structure, considering two sub-structures a and b , are computed as follows:

$$\Psi_s = \begin{Bmatrix} \Psi_i^{(a)} \\ \Psi_j \\ \Psi_i^{(b)} \end{Bmatrix} = \begin{Bmatrix} -\mathbf{K}_{ii}^{(a)-1} \mathbf{K}_{ij}^{(a)} \\ \mathbf{I}_{ij} \\ -\mathbf{K}_{ii}^{(b)-1} \mathbf{K}_{ij}^{(b)} \end{Bmatrix} \quad (7)$$

Branch modes \mathbf{x}_{Bj} are defined on a junction J between two substructures. They are solution of the eigen value problem of the global structure projected on the constraint static modes:

$$[\Psi_s^T \mathbf{K}_{tot} \Psi_s - \omega^2 \Psi_s^T \mathbf{M}_{tot} \Psi_s] \mathbf{x}_{Bj} = 0 \quad (8)$$

The basis \mathbf{X}_{Bj} of all branch modes \mathbf{x}_{Bj} spans the same subspace as the complete set of "constraint static modes" Ψ_s . The DMS consists in truncating the basis \mathbf{X}_{Bj} and keeping only the modes in the frequency range of interest.

Branch modes, once projected on substructure (s), can be written:

$$\mathbf{X}_{Bi}^{(s)} = \Psi_i^{(s)} \mathbf{X}_{Bj} \quad (9)$$

$$\mathbf{X}_{Bj}^{(s)} = \mathbf{I}_{jj} \mathbf{X}_{Bj} = \mathbf{X}_{Bj} \quad (10)$$

3.2. Fixed mode method

The fixed mode method is a primal method that separates, for each substructure (a), boundary DOFs $U_j^{(a)}$ and internal DOFs $U_i^{(a)}$. It projects the initial DOFs of the substructure (a) on a new smaller basis composed of truncated fixed modal DOFs $\eta_{FI}^{(a)}$ and truncated branch modes DOFs $\eta_B^{(a)}$, as follows:

$$\begin{Bmatrix} U_i^{(a)} \\ U_j^{(a)} \end{Bmatrix} = \begin{Bmatrix} \Phi_{FIi}^{(a)} & \mathbf{X}_{Bi}^{(a)} \\ \mathbf{0} & \mathbf{X}_{Bj} \end{Bmatrix} \begin{Bmatrix} \eta_{FI}^{(a)} \\ \eta_B^{(a)} \end{Bmatrix} \quad (11)$$

where $\Phi_{FIi}^{(a)}$ is a truncated basis composed of eigenmodes of the structure a assuming that the boundary nodes are held fixed, and $\left\{ \mathbf{X}_{Bi}^{(a)} \quad \mathbf{X}_{Bj} \right\}^T$ are the branch modes previously defined. Note that all the modes mentioned in this section are taken from the primal associated FEM with the same meshing.

3.3. Free mode method

The free mode method is a primal method that separates, for each substructure (a), boundary DOFs $U_j^{(a)}$ and internal DOFs $U_i^{(a)}$. It projects the initial DOFs of the substructure (a) on a new smaller basis composed of truncated free modal DOFs $\eta_{FR}^{(a)}$ and truncated branch modes DOFs $\eta_B^{(a)}$, as follows:

$$\begin{Bmatrix} U_i^{(a)} \\ U_j^{(a)} \end{Bmatrix} = \begin{Bmatrix} \Phi_{FRi}^{(a)} & \mathbf{X}_{Bi}^{(a)} \\ \Phi_{FRj}^{(a)} & \mathbf{X}_{Bj} \end{Bmatrix} \begin{Bmatrix} \eta_{FR}^{(a)} \\ \eta_B^{(a)} \end{Bmatrix} \quad (12)$$

where $\left\{ \Phi_{FRi}^{(a)} \quad \Phi_{FRj}^{(a)} \right\}^T$ is a truncated basis composed of eigenmodes of the structure a assuming that the boundary nodes are free, and $\left\{ \mathbf{X}_{Bi}^{(a)} \quad \mathbf{X}_{Bj} \right\}^T$ are the branch modes previously defined. Note that, once again all the modes mentioned in this section are taken from the primal associated FEM with the same meshing.

3.4. Projection of the stress field

The fixed and free mode method previously defined are primal methods. They project the displacement DOFs on a new basis, but they don't reduce the stress parameters used in a mixed formulation.

Considering the second line of the equation 5, we can express stress parameters in function of the displacement parameters of the corresponding stress, as follows:

$$\beta^{(a)} = -(\mathbf{H}^{(a)})^{-1} \mathbf{G}^{(a)} \mathbf{U}^{(a)} \quad (13)$$

That idea was already mentioned earlier in the possibility of transforming the mixed FEM into a "condensed" primal FEM. In our case, that method is only used for the reduction and the projection of the new basis for the stress.

Indeed, the projection of the stresses on a primal basis composed of fixed modes can now be express as follows:

$$\boldsymbol{\beta}^{(a)} = \left\{ \mathbf{P}^{(a)} \begin{Bmatrix} \boldsymbol{\Phi}_{FIi}^{(a)} \\ 0 \end{Bmatrix} \quad \mathbf{P}^{(a)} \begin{Bmatrix} \mathbf{X}_{Bi}^{(a)} \\ \mathbf{X}_{Bj} \end{Bmatrix} \right\} \begin{Bmatrix} \boldsymbol{\eta}_{FI}^{(a)} \\ \boldsymbol{\eta}_B^{(a)} \end{Bmatrix} \quad (14)$$

where $\mathbf{P}^{(a)} = -(\mathbf{H}^{(a)})^{-1}\mathbf{G}^{(a)}$. Those stress parameters can be considered as the stress resulting from the primal displacement modes.

In the same way, the projection of the stresses on a primal basis composed of free modes can be express as follows:

$$\boldsymbol{\beta}^{(a)} = \left\{ \mathbf{P}^{(a)} \begin{Bmatrix} \boldsymbol{\Phi}_{FRi}^{(a)} \\ \boldsymbol{\Phi}_{FRj}^{(a)} \end{Bmatrix} \quad \mathbf{P}^{(a)} \begin{Bmatrix} \mathbf{X}_{Bi}^{(a)} \\ \mathbf{X}_{Bj} \end{Bmatrix} \right\} \begin{Bmatrix} \boldsymbol{\eta}_{FR}^{(a)} \\ \boldsymbol{\eta}_B^{(a)} \end{Bmatrix} \quad (15)$$

3.5. Application to the mixed model

Considering the previous reduction methods we have described, we can now mix those methods to build various component mode synthesis for the mixed model. We consider 5 different types of reduction, and for each type we can use branch modes or not. For the sake of readability, the first part of the name is the projection of the displacements, the second is the projection of stresses and the third part makes the difference between a unique set of parameters for both displacements and stresses modes ("-1") or separated parameters for displacements and stresses ("-2"). For each method, we can choose to truncate the basis composed of branch modes ("-br" extension) or not (no extension). The table 1 summarizes the different mixed reductions we implemented.

The subscripts (U) and (β) are used in this part to make the difference between the parameters and components that refers to displacement fields and stresses fields, as they are mixed in the reduction.

3.5.1. Method Fix-Fix-1

In this section, we project the displacements on a basis composed of "fixed" modes and the stresses on a basis composed of "fixed" modes as well.

It is important to notice that the modal components $\boldsymbol{\eta}_{FI(U,\beta)}^a$ represents both the displacements and the stresses (hence the subscript (U, β)). In other words, the basis $\boldsymbol{\Phi}_{FIi(U)}^{(a)}$ composed of "fixed" modes describing the displacements is the same as the basis $\boldsymbol{\Phi}_{FIi(\beta)}^{(a)}$ describing the stresses (by projection) and they are both represented by the same component $\boldsymbol{\eta}_{FI(U,\beta)}^a$ for each mode.

We can also truncate the branch modes, and turn the reduction into a "Fix-Fix-1-br" reduction method. The reduction of the whole substructure a is given by:

$$\begin{Bmatrix} \mathbf{U}_i^{(a)} \\ \mathbf{U}_j^{(a)} \\ \boldsymbol{\beta}^{(a)} \end{Bmatrix} = \mathbf{T}^{(a)} \begin{Bmatrix} \boldsymbol{\eta}_{FI(U,\beta)}^{(a)} \\ \boldsymbol{\eta}_B^{(a)} \end{Bmatrix} \quad (16)$$

where

$$\mathbf{T}^{(a)} = \begin{Bmatrix} \boldsymbol{\Phi}_{FIi(U)}^{(a)} & \mathbf{X}_{Bi}^{(a)} \\ \mathbf{0} & \mathbf{X}_{Bj} \\ \mathbf{P}^{(a)} \begin{Bmatrix} \boldsymbol{\Phi}_{FIi(\beta)}^{(a)} \\ \mathbf{0} \end{Bmatrix} & \mathbf{P}^{(a)} \begin{Bmatrix} \mathbf{X}_{Bi}^{(a)} \\ \mathbf{X}_{Bj} \end{Bmatrix} \end{Bmatrix} \quad (17)$$

3.5.2. Method Fix-Fix-2

In this section, we also project the displacements on a basis composed of "fixed" modes and the stresses on a basis composed of "fixed" modes, as we did in the "Fix-Fix-1" method (see section 3.5.1).

Nevertheless, the difference is that the modal components that represent the displacements $\boldsymbol{\eta}_{FI(U)}^{(a)}$ are different from the ones representing the stresses $\boldsymbol{\eta}_{FI(\beta)}^{(a)}$. Even though the method is the same for the two basis $\boldsymbol{\Phi}_{FI i(U)}^{(a)}$ and $\boldsymbol{\Phi}_{FI i(\beta)}^{(a)}$, the truncations can be different and the components of the displacements and stresses are separated into respectively $\boldsymbol{\eta}_{FI(U)}^{(a)}$ and $\boldsymbol{\eta}_{FI(\beta)}^{(a)}$.

We can also truncate the branch modes, and turn the reduction into a "Fix-Fix-2-br". The reduction of the whole substructure a is given by:

$$\begin{Bmatrix} \mathbf{U}_i^{(a)} \\ \mathbf{U}_j^{(a)} \\ \boldsymbol{\beta}^{(a)} \end{Bmatrix} = \mathbf{T}^{(a)} \begin{Bmatrix} \boldsymbol{\eta}_{FI(U)}^{(a)} \\ \boldsymbol{\eta}_{FI(\beta)}^{(a)} \\ \boldsymbol{\eta}_B^{(a)} \end{Bmatrix} \quad (18)$$

where

$$\mathbf{T}^{(a)} = \begin{Bmatrix} \boldsymbol{\Phi}_{FI i(U)}^{(a)} & \mathbf{0} & \mathbf{X}_{Bi}^{(a)} \\ \mathbf{0} & \mathbf{0} & \mathbf{X}_{Bj}^{(a)} \\ \mathbf{0} & \mathbf{P}^{(a)} \begin{Bmatrix} \boldsymbol{\Phi}_{FI i(\beta)}^{(a)} \\ \mathbf{0} \end{Bmatrix} & \mathbf{P}^{(a)} \begin{Bmatrix} \mathbf{X}_{Bi}^{(a)} \\ \mathbf{X}_{Bj}^{(a)} \end{Bmatrix} \end{Bmatrix} \quad (19)$$

It is important to notice that the "Fix-Fix-2" method when not using "branch modes" is the same method as the one described in [37].

3.5.3. Method Fre-Fix-2

In this section, we project the displacements on a basis composed of "free" modes and the stresses on a basis composed of "fixed" modes.

In the same way as the "Fix-Fix-2" method, the modal component $\boldsymbol{\eta}_{FR(U)}^{(a)}$ representing the displacements and $\boldsymbol{\eta}_{FI(\beta)}^{(a)}$ representing the stresses are separated, which looks to be more logical in the case of this method, as the type of modes used for the projection are different with the fields reduced. The truncation can be different as well in this case.

We can also truncate the branch modes, and turn the reduction into a "Fre-Fix-2-br". The reduction of the whole substructure a is given by:

$$\begin{Bmatrix} \mathbf{U}_i^{(a)} \\ \mathbf{U}_j^{(a)} \\ \boldsymbol{\beta}^{(a)} \end{Bmatrix} = \mathbf{T}^{(a)} \begin{Bmatrix} \boldsymbol{\eta}_{FR(U)}^{(a)} \\ \boldsymbol{\eta}_{FI(\beta)}^{(a)} \\ \boldsymbol{\eta}_B^{(a)} \end{Bmatrix} \quad (20)$$

where

$$\mathbf{T}^{(a)} = \begin{Bmatrix} \boldsymbol{\Phi}_{FR i(U)}^{(a)} & \mathbf{0} & \mathbf{X}_{Bi}^{(a)} \\ \boldsymbol{\Phi}_{FR j(U)}^{(a)} & \mathbf{0} & \mathbf{X}_{Bj}^{(a)} \\ \mathbf{0} & \mathbf{P}^{(a)} \begin{Bmatrix} \boldsymbol{\Phi}_{FI i(\beta)}^{(a)} \\ \mathbf{0} \end{Bmatrix} & \mathbf{P}^{(a)} \begin{Bmatrix} \mathbf{X}_{Bi}^{(a)} \\ \mathbf{X}_{Bj}^{(a)} \end{Bmatrix} \end{Bmatrix} \quad (21)$$

3.5.4. Method Fre-Fre-1

In this section, we project the displacements on a basis composed of "free" modes and the stresses also on a basis composed of "free" modes as well.

In the same way as the "Fix-Fix-1" method (section 3.5.1), the modal components $\boldsymbol{\eta}_{FR(U,\beta)}^a$ represents both the displacements and the stresses (hence the subscript (U, β)). In other words, the basis $\left\{ \boldsymbol{\Phi}_{FRi(U)}^{(a)} \quad \boldsymbol{\Phi}_{FRj(U)}^{(a)} \right\}^T$ composed of "free" modes describing the displacements is the same as the basis $\left\{ \boldsymbol{\Phi}_{FRi(\beta)}^{(a)} \quad \boldsymbol{\Phi}_{FRj(\beta)}^{(a)} \right\}^T$ describing the stresses (by projection) and both displacements and stresses are represented by the same component $\boldsymbol{\eta}_{FR(U,\beta)}^a$ for each mode.

We can also truncate the branch modes, and turn the reduction into a "Fre-Fre-1-br" reduction method. The reduction of the whole substructure a is given by:

$$\begin{Bmatrix} \mathbf{U}_i^{(a)} \\ \mathbf{U}_j^{(a)} \\ \boldsymbol{\beta}^{(a)} \end{Bmatrix} = \mathbf{T}^{(a)} \begin{Bmatrix} \boldsymbol{\eta}_{FR(U,\beta)}^{(a)} \\ \boldsymbol{\eta}_B^{(a)} \end{Bmatrix} \quad (22)$$

where

$$\mathbf{T}^{(a)} = \begin{Bmatrix} \boldsymbol{\Phi}_{FRi(U)}^{(a)} & \mathbf{X}_{Bi}^{(a)} \\ \boldsymbol{\Phi}_{FRj(U)}^{(a)} & \mathbf{X}_{Bj} \\ \mathbf{P}^{(a)} \begin{Bmatrix} \boldsymbol{\Phi}_{FRi(\beta)}^{(a)} \\ \boldsymbol{\Phi}_{FRj(\beta)}^{(a)} \end{Bmatrix} & \mathbf{P}^{(a)} \begin{Bmatrix} \mathbf{X}_{Bi}^{(a)} \\ \mathbf{X}_{Bj} \end{Bmatrix} \end{Bmatrix} \quad (23)$$

3.5.5. Method Fre-Fre-2

In this section, we also project the displacements on a basis composed of "fixed" modes and the stresses on a basis composed of "fixed" modes, as we did in the "Fre-Fre-1" method (see section 3.5.4).

Nevertheless, the difference is that the modal components that represent the displacements $\boldsymbol{\eta}_{FR(U)}^{(a)}$ are different from the ones representing the stresses $\boldsymbol{\eta}_{FR(\beta)}^{(a)}$. Even though the method is the same for the two basis $\left\{ \boldsymbol{\Phi}_{FRi(U)}^{(a)} \quad \boldsymbol{\Phi}_{FRj(U)}^{(a)} \right\}^T$ and $\left\{ \boldsymbol{\Phi}_{FRi(\beta)}^{(a)} \quad \boldsymbol{\Phi}_{FRj(\beta)}^{(a)} \right\}^T$, the truncations can be different and the components representing each of the displacements and stresses are separated into respectively $\boldsymbol{\eta}_{FR(U)}^{(a)}$ and $\boldsymbol{\eta}_{FR(\beta)}^{(a)}$.

We can also truncate the branch modes, and turn the reduction into a "Fre-Fre-2-br". The reduction of the whole substructure a is given by:

$$\begin{Bmatrix} \mathbf{U}_i^{(a)} \\ \mathbf{U}_j^{(a)} \\ \boldsymbol{\beta}^{(a)} \end{Bmatrix} = \mathbf{T}^{(a)} \begin{Bmatrix} \boldsymbol{\eta}_{FR(U)}^{(a)} \\ \boldsymbol{\eta}_{FR(\beta)}^{(a)} \\ \boldsymbol{\eta}_B^{(a)} \end{Bmatrix} \quad (24)$$

where

$$\mathbf{T}^{(a)} = \begin{Bmatrix} \boldsymbol{\Phi}_{FRi(U)}^{(a)} & \mathbf{0} & \mathbf{X}_{Bi}^{(a)} \\ \boldsymbol{\Phi}_{FRj(U)}^{(a)} & \mathbf{0} & \mathbf{X}_{Bj} \\ \mathbf{0} & \mathbf{P}^{(a)} \begin{Bmatrix} \boldsymbol{\Phi}_{FRi(\beta)}^{(a)} \\ \boldsymbol{\Phi}_{FRj(\beta)}^{(a)} \end{Bmatrix} & \mathbf{P}^{(a)} \begin{Bmatrix} \mathbf{X}_{Bi}^{(a)} \\ \mathbf{X}_{Bj} \end{Bmatrix} \end{Bmatrix} \quad (25)$$

It should be noted as well that, the projection using some eigenmodes of the primal equivalent FEM, our method requires to build both primal and mixed assemblage at the same time for each structure we study, as all the reduction of the mixed FEM comes from the primal associated FEM. Of course, both models use the same theory and same meshing to link them together.

3.6. Assembly

After reducing the sub-structures, the next step of the sub-structuring reduction method is to assemble them. In this section, we implement the assembly for two sub-structures a and b .

There exists a wide range of methods to do it as hybrid, implicit or explicit methods, primal or dual connexions with either strong or weak links. In the present work, we aim to assemble the two sub-structures a and b with an explicit strong form on the displacement side as follows:

$$\mathbf{U}_j^{(a)} = \mathbf{U}_j^{(b)} = \mathbf{U}_j \quad (26)$$

The connexion of the stresses is implicit and contained into the equation 13.

This assembly method leads to different formulations, depending on the method we use for the projection of the displacement field ("free" mode and "fixed mode method").

3.6.1. "Free" mode method on displacements

The use of free modes for the projection of displacements is contained in the methods Fre-Fix-2 (3.5.3), Fre-Fre-1 (3.5.4) and Fre-Fre-2 (3.5.5). In this case, the equation 26 leads to the following form:

$$\Phi_{FRj(U)}^{(a)} \boldsymbol{\eta}_{FR(U)}^{(a)} + \mathbf{X}_{Bj}^{(a)} \boldsymbol{\eta}_B^{(a)} = \Phi_{FRj(U)}^{(b)} \boldsymbol{\eta}_{FR(U)}^{(b)} + \mathbf{X}_{Bj}^{(b)} \boldsymbol{\eta}_B^{(b)} \quad (27)$$

As $\mathbf{X}_{Bj}^{(a)} = \mathbf{X}_{Bj}^{(b)} = \mathbf{X}_{Bj}$, we now have:

$$\boldsymbol{\eta}_B^{(b)} = (\mathbf{X}_{Bj}^{-1} \Phi_{FRj(U)}^{(a)}) \boldsymbol{\eta}_{FR(U)}^{(a)} + \boldsymbol{\eta}_B^{(a)} + (-\mathbf{X}_{Bj}^{-1} \Phi_{FRj(U)}^{(b)}) \boldsymbol{\eta}_{FR(U)}^{(b)} \quad (28)$$

Fre-Fix-2 For the method "Fre-Fix-2", the reduction of the assembly of the structure $(a + b)$ is then given by:

$$\begin{Bmatrix} \mathbf{U}_i^{(a)} \\ \mathbf{U}_j \\ \mathbf{U}_i^{(b)} \\ \boldsymbol{\beta}^{(a)} \\ \boldsymbol{\beta}^{(b)} \end{Bmatrix} = \mathbf{T} \begin{Bmatrix} \boldsymbol{\eta}_{FR(U)}^{(a)} \\ \boldsymbol{\eta}_{FI(\beta)}^{(b)} \\ \boldsymbol{\eta}_B^{(a)} \\ \boldsymbol{\eta}_{FR(U)}^{(b)} \\ \boldsymbol{\eta}_{FI(\beta)}^{(b)} \end{Bmatrix} \quad (29)$$

where

$$\mathbf{T} = \begin{Bmatrix} \Phi_{FRi(U)}^{(a)} & \mathbf{0} & \mathbf{X}_{Bj}^{(a)} & \mathbf{0} & \mathbf{0} \\ \Phi_{FRj(U)}^{(a)} & \mathbf{0} & \mathbf{X}_{Bj} & \mathbf{0} & \mathbf{0} \\ \mathbf{0} & \mathbf{0} & \mathbf{X}_{Bj}^{(b)} & \Phi_{FRi(U)}^{(b)} & \mathbf{0} \\ \mathbf{0} & \mathbf{P}^{(a)} \begin{Bmatrix} \Phi_{FIi(\beta)}^{(a)} \\ \mathbf{0} \end{Bmatrix} & \mathbf{P}^{(a)} \begin{Bmatrix} \mathbf{X}_{Bj}^{(a)} \\ \mathbf{X}_{Bj} \end{Bmatrix} & \mathbf{0} & \mathbf{0} \\ \mathbf{0} & \mathbf{0} & \mathbf{P}^{(b)} \begin{Bmatrix} \mathbf{X}_{Bi}^{(b)} \\ \mathbf{X}_{Bj} \end{Bmatrix} & \mathbf{0} & \mathbf{P}^{(b)} \begin{Bmatrix} \Phi_{FIi(\beta)}^{(b)} \\ \mathbf{0} \end{Bmatrix} \end{Bmatrix} \quad (30)$$

Fre-Fre-1 For the method "Fre-Fre-1", the reduction of the assembly of the structure $(a + b)$ is then given by:

$$\begin{Bmatrix} \mathbf{U}_i^{(a)} \\ \mathbf{U}_j \\ \mathbf{U}_i^{(b)} \\ \boldsymbol{\beta}^{(a)} \\ \boldsymbol{\beta}^{(b)} \end{Bmatrix} = \mathbf{T} \begin{Bmatrix} \boldsymbol{\eta}_{FR(U,\beta)}^{(a)} \\ \boldsymbol{\eta}_B^{(a)} \\ \boldsymbol{\eta}_{FR(U,\beta)}^{(b)} \end{Bmatrix} \quad (31)$$

where

$$T = \left\{ \begin{array}{ccc} \Phi_{FRi(U)}^{(a)} & \mathbf{X}_{Bj}^{(a)} & \mathbf{0} \\ \Phi_{FRj(U)}^{(a)} & \mathbf{X}_{Bj} & \mathbf{0} \\ \mathbf{0} & \mathbf{X}_{Bj}^{(b)} & \Phi_{FRi(U)}^{(b)} \\ \mathbf{P}^{(a)} \left\{ \begin{array}{c} \Phi_{FRi(\beta)}^{(a)} \\ \Phi_{FRj(\beta)}^{(a)} \end{array} \right\} & \mathbf{P}^{(a)} \left\{ \begin{array}{c} \mathbf{X}_{Bj}^{(a)} \\ \mathbf{X}_{Bj} \end{array} \right\} & \mathbf{0} \\ \mathbf{0} & \mathbf{P}^{(b)} \left\{ \begin{array}{c} \mathbf{X}_{Bi}^{(b)} \\ \mathbf{X}_{Bj} \end{array} \right\} & \mathbf{P}^{(b)} \left\{ \begin{array}{c} \Phi_{FRi(\beta)}^{(b)} \\ \Phi_{FRj(\beta)}^{(b)} \end{array} \right\} \end{array} \right\} \quad (32)$$

Fre-Fre-2 For the method "Fre-Fre-2", the reduction of the assembly of the structure $(a + b)$ is then given by:

$$\left\{ \begin{array}{c} \mathbf{U}_i^{(a)} \\ \mathbf{U}_j \\ \mathbf{U}_i^{(b)} \\ \beta^{(a)} \\ \beta^{(b)} \end{array} \right\} = T \left\{ \begin{array}{c} \eta_{FR(U)}^{(a)} \\ \eta_{FR(\beta)}^{(b)} \\ \eta_B^{(a)} \\ \eta_{FR(U)}^{(b)} \\ \eta_{FR(\beta)}^{(b)} \end{array} \right\} \quad (33)$$

where

$$T = \left\{ \begin{array}{ccccc} \Phi_{FRi(U)}^{(a)} & \mathbf{0} & \mathbf{X}_{Bj}^{(a)} & \mathbf{0} & \mathbf{0} \\ \Phi_{FRj(U)}^{(a)} & \mathbf{0} & \mathbf{X}_{Bj} & \mathbf{0} & \mathbf{0} \\ \mathbf{0} & \mathbf{0} & \mathbf{X}_{Bj}^{(b)} & \Phi_{FRi(U)}^{(b)} & \mathbf{0} \\ \mathbf{0} & \mathbf{P}^{(a)} \left\{ \begin{array}{c} \Phi_{FRi(\beta)}^{(a)} \\ \Phi_{FRj(\beta)}^{(a)} \end{array} \right\} & \mathbf{P}^{(a)} \left\{ \begin{array}{c} \mathbf{X}_{Bj}^{(a)} \\ \mathbf{X}_{Bj} \end{array} \right\} & \mathbf{0} & \mathbf{0} \\ \mathbf{0} & \mathbf{0} & \mathbf{P}^{(b)} \left\{ \begin{array}{c} \mathbf{X}_{Bi}^{(b)} \\ \mathbf{X}_{Bj} \end{array} \right\} & \mathbf{0} & \mathbf{P}^{(b)} \left\{ \begin{array}{c} \Phi_{FRi(\beta)}^{(b)} \\ \Phi_{FRj(\beta)}^{(b)} \end{array} \right\} \end{array} \right\} \quad (34)$$

3.6.2. "Fixed" mode method on displacements

The use of free modes for the projection of displacements is contained in the methods Fix-Fix-1 (3.5.1) and Fix-Fix-2 (3.5.2). In this case, the equation 26 leads to the following form:

$$\mathbf{X}_{Bj}^{(a)} = \mathbf{X}_{Bj}^{(b)} = \mathbf{X}_{Bj} \quad (35)$$

Fix-Fix-1 For the method "Fix-Fix-1", the reduction of the assembly of the structure $(a + b)$ is then given by:

$$\left\{ \begin{array}{c} \mathbf{U}_i^{(a)} \\ \mathbf{U}_j \\ \mathbf{U}_i^{(b)} \\ \beta^{(a)} \\ \beta^{(b)} \end{array} \right\} = T \left\{ \begin{array}{c} \eta_{FI(U,\beta)}^{(a)} \\ \eta_B^{(a)} \\ \eta_{FI(U,\beta)}^{(b)} \end{array} \right\} \quad (36)$$

where

$$T = \begin{pmatrix} \Phi_{FI i(U)}^{(a)} & \mathbf{0} & \mathbf{0} & \mathbf{0} \\ \mathbf{0} & \mathbf{0} & \mathbf{0} & \mathbf{0} \\ \mathbf{0} & \mathbf{0} & \mathbf{0} & \Phi_{FI i(U)}^{(b)} \\ P^{(a)} \begin{Bmatrix} \Phi_{FI i(\beta)}^{(a)} \\ \mathbf{0} \end{Bmatrix} & P^{(a)} \begin{Bmatrix} X_{Bj}^{(a)} \\ X_{Bj} \\ X_{Bj}^{(b)} \end{Bmatrix} & \mathbf{0} & \mathbf{0} \\ \mathbf{0} & P^{(b)} \begin{Bmatrix} X_{Bi}^{(b)} \\ X_{Bj} \end{Bmatrix} & P^{(b)} \begin{Bmatrix} \Phi_{FI i(\beta)}^{(b)} \\ \mathbf{0} \end{Bmatrix} \end{pmatrix} \quad (37)$$

Fix-Fix-2 For the method "Fix-Fix-2", the reduction of the assembly of the structure $(a + b)$ is then given by:

$$\begin{Bmatrix} U_i^{(a)} \\ U_j \\ U_i^{(b)} \\ \beta^{(a)} \\ \beta^{(b)} \end{Bmatrix} = T \begin{Bmatrix} \eta_{FI(U)}^{(a)} \\ \eta_{FI(\beta)}^{(b)} \\ \eta_B^{(a)} \\ \eta_{FI(U)}^{(b)} \\ \eta_{FI(\beta)}^{(b)} \end{Bmatrix} \quad (38)$$

where

$$T = \begin{pmatrix} \Phi_{FI i(U)}^{(a)} & \mathbf{0} & \mathbf{0} & \mathbf{0} & \mathbf{0} \\ \mathbf{0} & \mathbf{0} & \mathbf{0} & \mathbf{0} & \mathbf{0} \\ \mathbf{0} & \mathbf{0} & \mathbf{0} & \Phi_{FI i(U)}^{(b)} & \mathbf{0} \\ \mathbf{0} & P^{(a)} \begin{Bmatrix} \Phi_{FI i(\beta)}^{(a)} \\ \mathbf{0} \end{Bmatrix} & P^{(a)} \begin{Bmatrix} X_{Bj}^{(a)} \\ X_{Bj} \end{Bmatrix} & \mathbf{0} & \mathbf{0} \\ \mathbf{0} & \mathbf{0} & P^{(b)} \begin{Bmatrix} X_{Bi}^{(b)} \\ X_{Bj} \end{Bmatrix} & \mathbf{0} & P^{(b)} \begin{Bmatrix} \Phi_{FI i(\beta)}^{(b)} \\ \mathbf{0} \end{Bmatrix} \end{pmatrix} \quad (39)$$

For each method, we can choose to truncate the basis composed of branch modes (method with "-br" extension) or not.

The figure 1 summarizes the calculation of the dynamic response with the use of the substructuring method (the subscripts *pri*, *mix* and *red* representing respectively the primal, mixed, and mixed reduced matrix).

In the next sections, we use a simple example with two sub-structures to check the convergence of those methods in function of the truncation of the eigenmodes of each sub-structure, and then we will check the influence of the truncation of the branch modes.

4. NUMERICAL EXAMPLE: ASSEMBLING TWO KIRCHHOFF-LOVE THIN MIXED PLATE

This section focus on the convergence of DM-FEMs using the different methods described in section 3, depending on the number of modes kept in the truncation for displacement fields, the stress fields

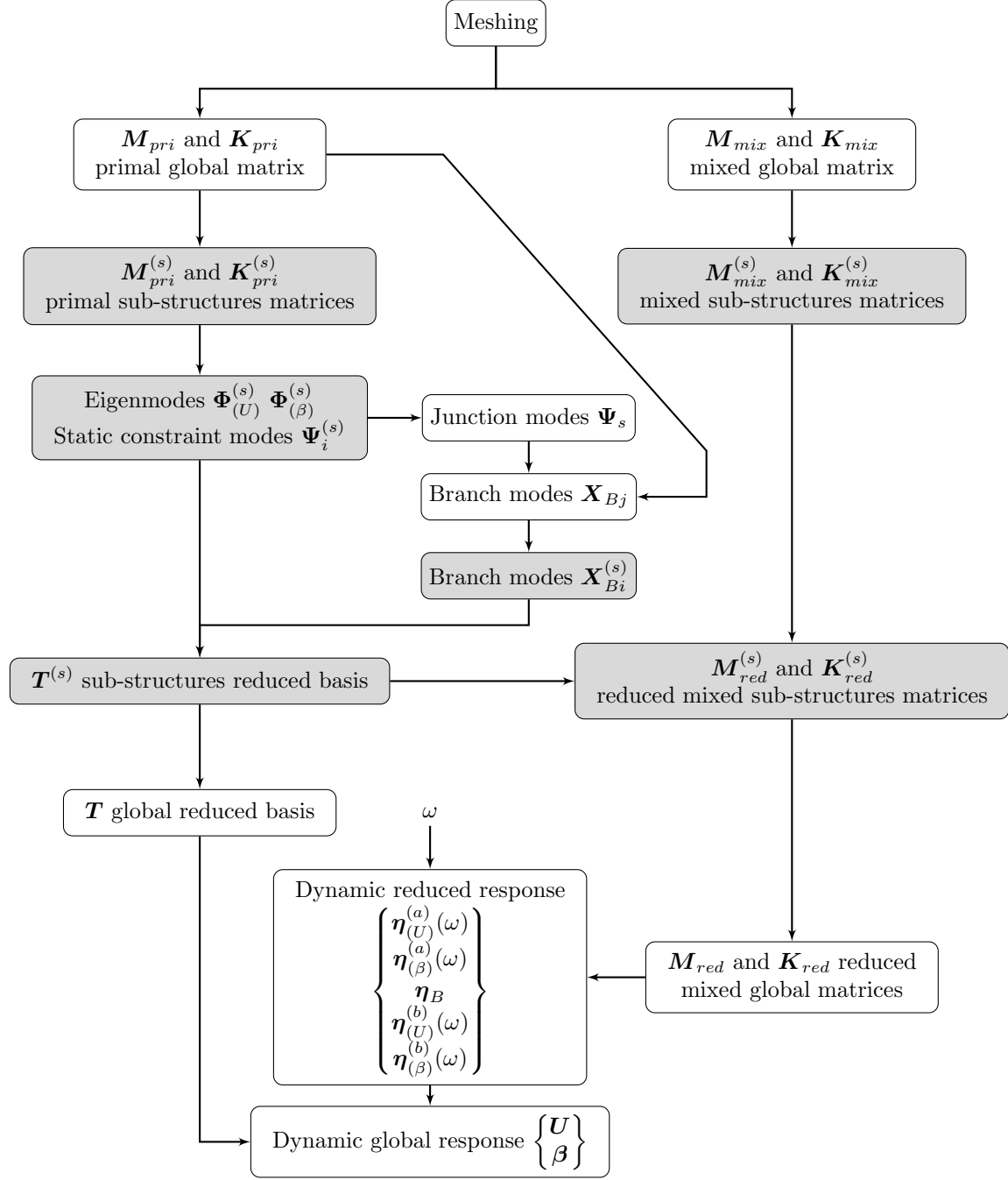


Figure 1: Computation of the dynamic response of the global structure using the sub-structuring method (global structure level, sub-structure (s) level). Each block needs all the input to be computed

and the truncation of the branch modes. It necessitates to choose a structure example and a corresponding mechanical theory. We decide to study a simple structure with two main plates built with a DM-FEM based on the KL thin plate theory. The three first subsections describe respectively the structure example, the construction of the model and the checking method.

Then, in the next subsections, we calculate the results of the dynamic response of the global structure with the sub-structuring methods for different truncations of the eigenmodes of the sub-structures (see Table 2). We first decide to truncate the "internal" eigenmodes of each sub-structures, keeping the junction as is, and then study the influence of the truncation of the branch modes.

The table 2 summarizes the different truncations we tested for each sub-structuring method and compare it to the non-reduced method parameters.

4.1. Structure example

The structure studied in this part is composed of two different plates, meshed with KL triangular DM-FEM described in the next section 4.2. It is made of steel (see characteristics in table 3) and we choose a thickness of $1e^{-3}m$. That example is shown in figure 2.

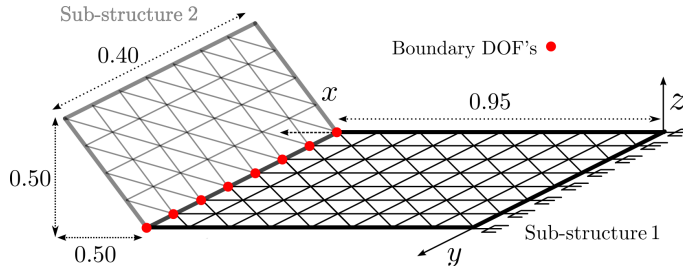


Figure 2: Double structured thin plate built with KL triangular mixed elements

The global structure is composed of 922 elements whilst the first plate is composed of 414 elements and the second plate of 510 elements. The first plate is clamped on one edge (102 DOFs clamped) and the junction is composed of 102 boundary DOFs. The table 4 summarise the elements and DOFs characteristics of the test structure and substructures.

4.2. Mixed finite element for Kirchoff-Love Thin Plate

In this part, we aim at detailing the specificities of the DM-FEM based on the KL thin plate theory we used as our example. The KL theory [49, 58] is a theory for thin plates that only focus on bending and twisting phenomenons. The mixed formulation explained in section 2 necessitates a few explanation in the case of such a theory. The details of the specific DM-FEM for thin KL plate (of thickness t) used here is given in this section.

4.2.1. Displacements and strain

The plate displacement considers w the transverse displacement, and θ_x and θ_y the normal rotation around the $-x$ and $-y$ axis. The theory of KL is C^1 continuous, and assumes that the 2 rotations

Table 2: Different truncation of internal modes for each DMS and sub-structuring method (number of modes per sub-structure)

Sub-structuring method	Name	U modes per sub-structures	β modes	Branch modes	DOFs
None	Primal non-reduced method				2958
None	Mixed non-reduced method				11256
Fix-Fix-1	5-5	5	5	Full	112
Fix-Fix-1	10-10	10	10	Full	122
Fix-Fix-1	20-20	20	20	Full	142
Fix-Fix-1	40-40	40	40	Full	182
Fix-Fix-1	60-60	60	60	Full	222
Fix-Fix-1	80-80	80	80	Full	262
Fix-Fix-2	5-5	5	5	Full	122
Fix-Fix-2	10-10	10	10	Full	142
Fix-Fix-2	20-20	20	20	Full	182
Fix-Fix-2	40-40	40	40	Full	262
Fix-Fix-2	60-60	60	60	Full	342
Fix-Fix-2	80-80	80	80	Full	422
Fre-Fix-2	20-20	20	20	Full	182
Fre-Fix-2	40-40	40	40	Full	262
Fre-Fix-2	60-60	60	60	Full	342
Fre-Fix-2	80-80	80	80	Full	422
Fre-Fix-2	150-150	150	150	Full	702
Fre-Fix-2	200-200	200	200	Full	902
Fre-Fre-1	20-20	20	20	Full	142
Fre-Fre-1	40-40	40	40	Full	182
Fre-Fre-1	60-60	60	60	Full	222
Fre-Fre-1	80-80	80	80	Full	262
Fre-Fre-1	100-100	100	100	Full	302
Fre-Fre-2	20-20	20	20	Full	182
Fre-Fre-2	40-40	40	40	Full	262
Fre-Fre-2	60-60	60	60	Full	342
Fre-Fre-2	80-80	80	80	Full	422
Fre-Fre-2	100-100	100	100	Full	502
Fre-Fre-2	150-150	150	150	Full	02

Table 3: Steel characteristics

Young Modulus (Pa)	2.1×10^{11}
Poisson ratio	0.33
Density ($kg.m^{-3}$)	7.5×10^3

Table 4: Characteristics of the test structure for the convergence study

Plate	Elements	DOFs	displacement DOFs	Generalized stress DOFs	Boundary DOFs
Global structure	922	11256	2958	8298	/
Sub-structure 1	414	5064	1338	3726	102
Sub-structure 2	510	6294	1722	4572	102

θ_x and θ_y depend on the transverse displacement w . Thus the interpolation for the chosen 3-node triangular element in function of the 9 nodal displacements $\{w_i \ \theta_{xi} \ \theta_{yi}\}_{(i=1,2,3)}$ is as follows:

$$\mathbf{u}_i = \begin{Bmatrix} w \\ \theta_x \\ \theta_y \end{Bmatrix} = \begin{Bmatrix} w \\ \frac{\partial w}{\partial y} \\ -\frac{\partial w}{\partial x} \end{Bmatrix} = \mathbf{N}\mathbf{U} = \begin{Bmatrix} N_1 & N_2 & \dots & N_9 \\ \frac{\partial N_1}{\partial y} & \frac{\partial N_2}{\partial y} & \dots & \frac{\partial N_9}{\partial y} \\ -\frac{\partial N_1}{\partial x} & -\frac{\partial N_2}{\partial x} & \dots & -\frac{\partial N_9}{\partial x} \end{Bmatrix} \mathbf{U} \quad (40)$$

The strain is derived from the displacement and given by:

$$\mathbf{e}_{ij} = \begin{Bmatrix} \epsilon_{xx} \\ \epsilon_{yy} \\ \gamma_{xy} \end{Bmatrix} = \mathbf{D} \mathbf{u}_i = \begin{Bmatrix} 0 & 0 & \frac{\partial}{\partial x} \\ 0 & -\frac{\partial}{\partial y} & 0 \\ 0 & \frac{\partial}{\partial x} & \frac{\partial}{\partial y} \end{Bmatrix} \mathbf{N}\mathbf{U} \quad (41)$$

4.2.2. Generalized stress

In the case of a plate theory, we actually discretize generalized stress, as follows:

$$\boldsymbol{\sigma}_{ij} = \begin{Bmatrix} M_x \\ M_y \\ M_{xy} \end{Bmatrix} = \mathbf{P}\boldsymbol{\beta} = \begin{Bmatrix} 1 & x & y & 0 & 0 & 0 & 0 & 0 & 0 \\ 0 & 0 & 0 & 1 & x & y & 0 & 0 & 0 \\ 0 & 0 & 0 & 0 & 0 & 0 & 1 & x & y \end{Bmatrix} \begin{Bmatrix} \beta_1 \\ \beta_2 \\ \vdots \\ \beta_9 \end{Bmatrix} \quad (42)$$

where $\{M_x, M_y, M_{xy}\}^T$ represents the bending and twisting moments. The elastic compliance matrix is given by:

$$\mathbf{S}_{ijkl} = \begin{Bmatrix} \frac{12}{Et^3} & -\frac{12\nu}{Et^3} & 0 \\ -\frac{12\nu}{Et^3} & \frac{12}{Et^3} & 0 \\ 0 & 0 & \frac{24(1+\nu)}{Et^3} \end{Bmatrix} \quad (43)$$

4.2.3. Variational function and mixed finite element formulation

The matrix development 5 remains the same, but the expression of the constitutive matrices 6 changes with the plate theory implementation:

$$\mathbf{M} = \iint_S \mathbf{N}^T \mathbf{m} \mathbf{N} dS, \quad \mathbf{G} = \iint_S \mathbf{P}^T \mathbf{D} \mathbf{N} dS, \quad \mathbf{H} = \iint_S -\mathbf{P}^T \mathbf{S} \mathbf{P} dS \quad (44)$$

where

$$\mathbf{m} = \rho \begin{pmatrix} t & 0 & 0 \\ 0 & \frac{t^3}{12} & 0 \\ 0 & 0 & \frac{t^3}{12} \end{pmatrix} \quad (45)$$

4.3. Checking Method

This section focuses on the convergence of the reduced DM-FEM in comparison to the DM-FEM with no reduction (the DM-FEM having already converged with the meshing used). We calculate the dynamic response of the global structure with the sub-structuring method (see section 3) and for different truncations, and compare it to the non-reduced dynamic response. The checking procedure contains 2 part. The first part concerns the relative error between the eigenfrequencies of the each mode i of the global structure as described in the following equation:

$$\epsilon_{i,\text{red/mix}} = \frac{\text{abs}(f_{i,\text{mixed reduced}} - f_{i,\text{mixed}})}{f_{i,\text{mixed}}} \quad (46)$$

The second part concerns the shape of the modes and uses the Mac criterion as follows:

$$MAC(i, j) = \frac{(\mathbf{X}_i^T \mathbf{X}_j)^2}{(\mathbf{X}_i^T \mathbf{X}_i)(\mathbf{X}_j^T \mathbf{X}_j)} \quad (47)$$

with X_i the shape of the mode i of the primal FEM and X_j the shape of the mode j of the mixed FEM, taking into consideration only both displacement and stress fields.

4.4. Convergence study: truncation of the internal displacement and stress modes

The results are explained with 2 graphics (figures 3, 5, 7 and 9), and figures 4, 6, 8 and 10) for each truncation, and the table 5 summarizing the results of all of them.

The first graphic describes the relative error (equation 46) on the eigenfrequencies in function of the mode i and compare it to an arbitrary limit of 3%. Each marker gives an insight of the MAC criterion (equation 47) of the mode i , as follows:

- black marker: $MAC \geq 0.8$ ("good" criterion)
- grey marker: $0.5 \leq MAC < 0.8$ ("medium" criterion)
- white marker: $MAC < 0.5$ ("bad" criterion)

The second graphic shows the matrix of the MAC criterion comparing the mixed non-reduced model to the mixed reduced model, so as to focus on the form of the modes.

The table 5 summarizes the results for each sub-structuring method and for the different truncations, focusing on two major points.

Indeed, most of the results comes with a good representation (frequency and form) for low frequencies until a convergence limit frequency that increases with the number of modes kept in the truncation. The table shows that limit, in terms of mode number and frequency.

Nevertheless, depending on the method and the truncation, it sometimes remains some modes with one of the two criteria (relative error, MAC criterion or sometimes both) that is "medium" or even "bad" for some modes (see section 4.3). We call them "singular modes". The table depicts the number and density of "singular modes" among the frequency band assumed converged. Depending on that density, it can deteriorate the quality of the method, even if the frequency band is good, hence the importance of mentioning it.

Table 5: Results for different truncations of "internal" modes, using the mixed DMS sub-structuring methods

Method	Name	Figures		Limit		Singular modes		DOFs
		error	MAC	mode	freq (Hz)	nb	%	
Primal non-reduced method								2958
Mixed non-reduced method								11256
Fix-Fix-1or2	5-5	3a	4a	12	33	0	0%	112 or 122
Fix-Fix-1or2	10-10	3b	4b	22	70	0	0%	122 or 142
Fix-Fix-1or2	20-20	3c	4c	42	149	2	4.8%	142 or 182
Fix-Fix-1or2	40-40	3d	4d	76	290	2	2.6%	182 or 262
Fix-Fix-1or2	60-60	3e	4e	113	447	6	5.3%	222 or 342
Fix-Fix-1or2	80-80	3f	4f	147	580	4	2.7%	262 or 422
Fre-Fix-2	20-20	5a	6a	34	110	23	68%	182
Fre-Fix-2	40-40	5b	6b	66	242	42	64%	262
Fre-Fix-2	60-60	5c	6c	102	385	59	58%	342
Fre-Fix-2	80-80	5d	6d	136	530	68	50%	422
Fre-Fix-2	150-150	5e	6e	260	1100	148	57%	702
Fre-Fix-2	200-200	5f	6f	325	1500	201	62%	902
Fre-Fre-1	20-20	7a	8a	27	90	17	63%	142
Fre-Fre-1	40-40	7b	8b	65	241	29	45%	182
Fre-Fre-1	60-60	7c	8c	89	338	26	29%	222
Fre-Fre-1	80-80	7d	8d	131	518	52	40%	262
Fre-Fre-1	100-100	7e	8e	142	568	62	44%	302
Fre-Fre-2	20-20	9a	10a	27	90	21	78%	182
Fre-Fre-2	40-40	9b	10b	65	241	18	28%	262
Fre-Fre-2	60-60	9c	10c	89	338	7	8%	342
Fre-Fre-2	80-80	9d	10d	131	518	21	16%	422
Fre-Fre-2	100-100	9e	10e	165	661	22	13%	502
Fre-Fre-2	150-150	9f	10f	239	992	20	8%	702

4.4.1. Fix-Fix-1 and Fix-Fix-2 method

The results are shown in figure 3 (relative error and insight of the MAC criterion), figures 4 (matrix of the MAC criterion) and table 5.

The Fix-Fix-2 method, when not truncating the branch modes, is the same as the method described in [37] and it provided good results. This paper proposes another method with "fixed modes" for both displacement and stress parameters, called "Fix-Fix-1", but the difference is made with the internal modal DOFs $\boldsymbol{\eta}_{FI(U,\beta)}^{(a)}$ in the reduced basis that are the same for displacements and stresses. The results obtained for the new Fix-Fix-1 are exactly the same as for the Fix-Fix-2 method.

The results depicted in the table 5 are very good and allow to increase a lot the truncation and still keep good results. The representation for low frequencies is good until the limit frequency and the limit is higher than for the other methods with the same truncation. However, the density of "singular modes" among the converged frequency band, is small less than 6% for all the truncations.

4.4.2. Fre-Fix-2 method

The results are shown in figure 5 (relative error and insight of the MAC criterion), figures 6 (matrix of the MAC criterion) and table 5.

The Fre-Fix-2 method does not show a good efficiency. Indeed, despite the limit frequency almost as high as the Fix-Fix-1or2 method, the density of singular modes is more than 50% for every truncation, which is too much to consider the results conclusive. In fact, the notion of "limit frequency" is not even relevant considering that more than half of the frequency band supposedly converged has either one of the two criteria or sometimes both criteria that have not converged.

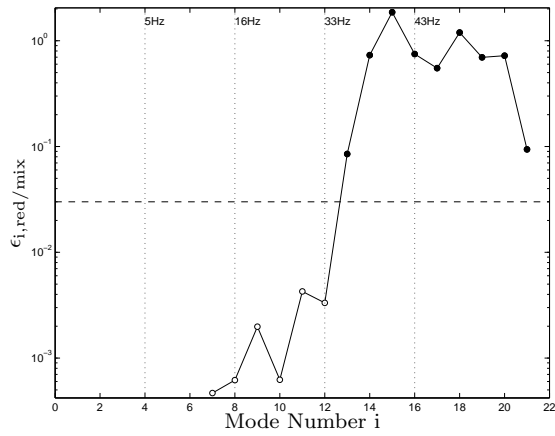
4.4.3. Fre-Fre-1 method

The results are shown in figure 7 (relative error and insight of the MAC criterion), figures 8 (matrix of the MAC criterion) and table 5.

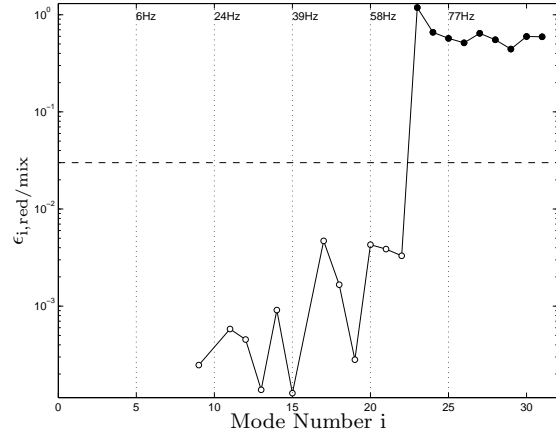
The Fre-Fre-1 method shows average results. The limit frequency is not as high as for the for the Fix-Fix-1or2 method, and the density of "singular modes" is also higher than for the Fix-Fix1or2. Nevertheless, that density is smaller than for the Fre-Fix-2. It appears that, apart from a high truncation (20-20 or smaller), that density is about 40%, which is a bit better than the results of the Fre-Fix-2 method. Furthermore, when comparing the overall results for the Fre-Fre-2 method (figures 7 and 8) and the Fre-Fix-2 method (figures 5 and 6) shows that the "singular modes" of the Fre-Fix-2 method are a bit worse than the ones of the Fre-Fre-2 methods (in terms of MAC criterion). All in all, the relevance of this method is small, although better than the Fre-Fix-2 method.

4.4.4. Fre-Fre-2 method

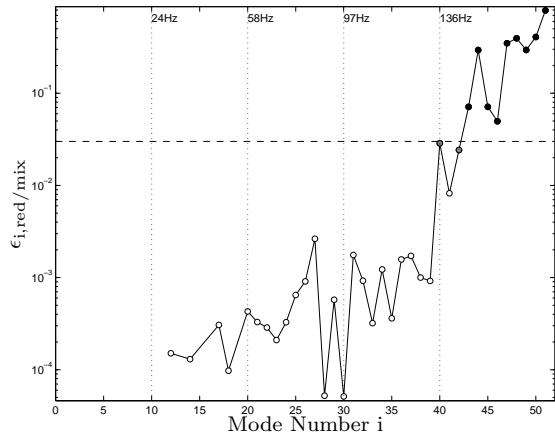
The results are shown in figure 9 (relative error and insight of the MAC criterion), figures 10 (matrix of the MAC criterion) and table 5.



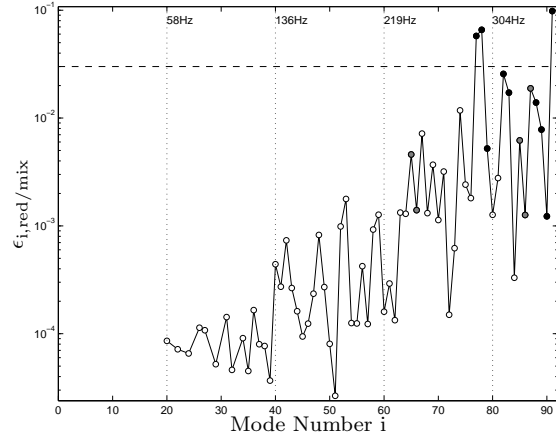
(a) 5-5



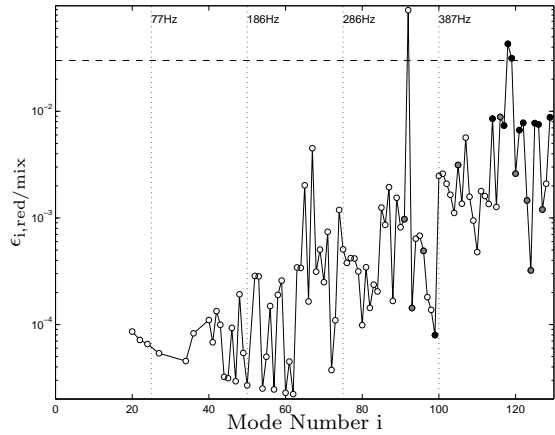
(b) 10-10



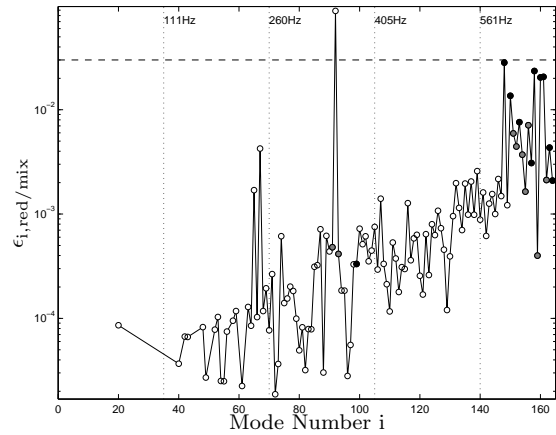
(c) 20-20



(d) 40-40



(e) 60-60



(f) 80-80

Figure 3: Relative error on the eigenfrequencies $\epsilon_{i,\text{red}/\text{mix}}$ in function of the mode i and insight of the MAC criterion for each modes (method Fix-Fix-1or2: truncations: a:5-5, b:10-10, c:20-20, d:40-40, e:60-60, f:80-80)

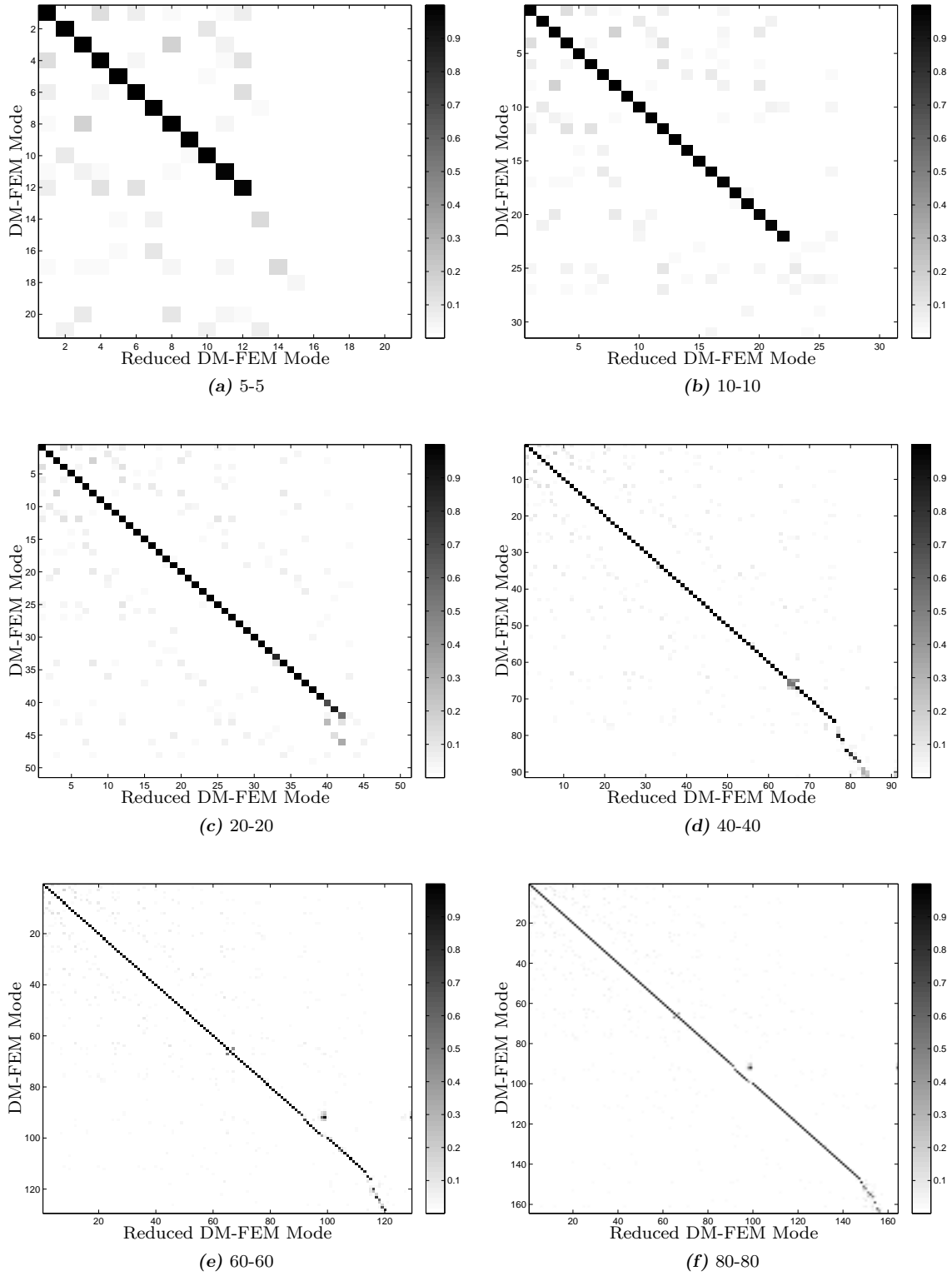
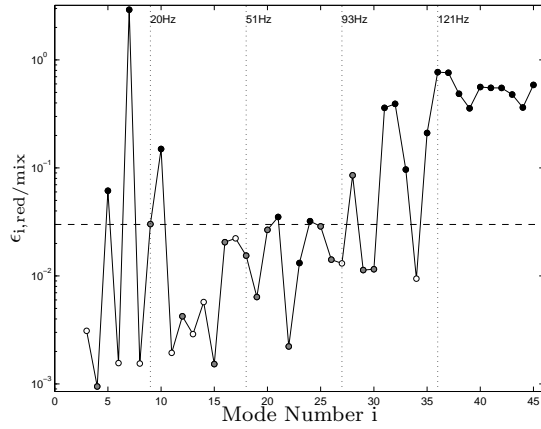
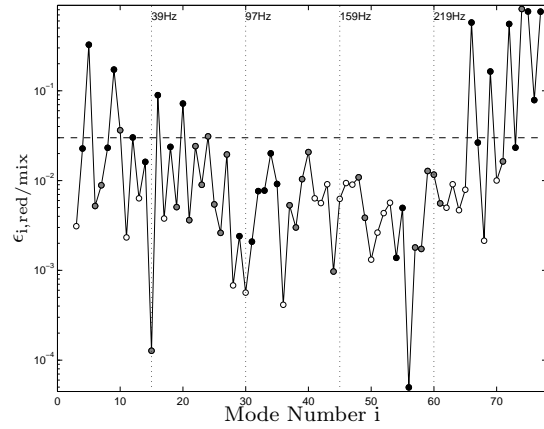


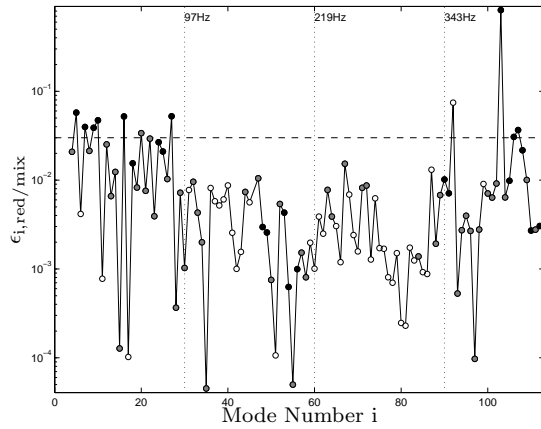
Figure 4: MAC criterion for each modes (method Fix-Fix-1or2: truncations: a:5-5, b:10-10, c:20-20, d:40-40, e:60-60, f:80-80)



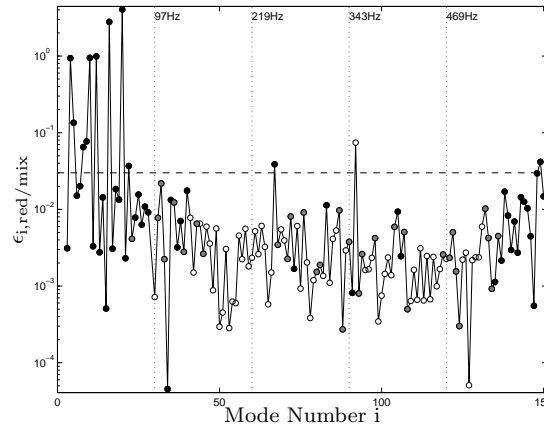
(a) 20-20



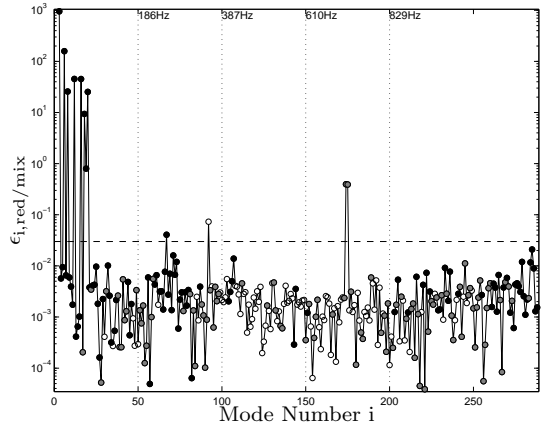
(b) 40-40



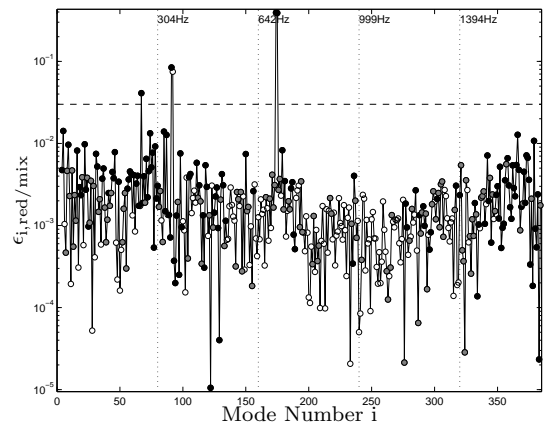
(c) 60-60



(d) 80-80



(e) 150-150



(f) 200-200

Figure 5: Relative error on the eigenfrequencies $\epsilon_{i,\text{red}/\text{mix}}$ in function of the mode i and insight of the MAC criterion for each modes (method Fre-Fix-2: truncations: a:20-20, b:40-40, c:60-60, d:80-80, e:150-150, f:200-200)

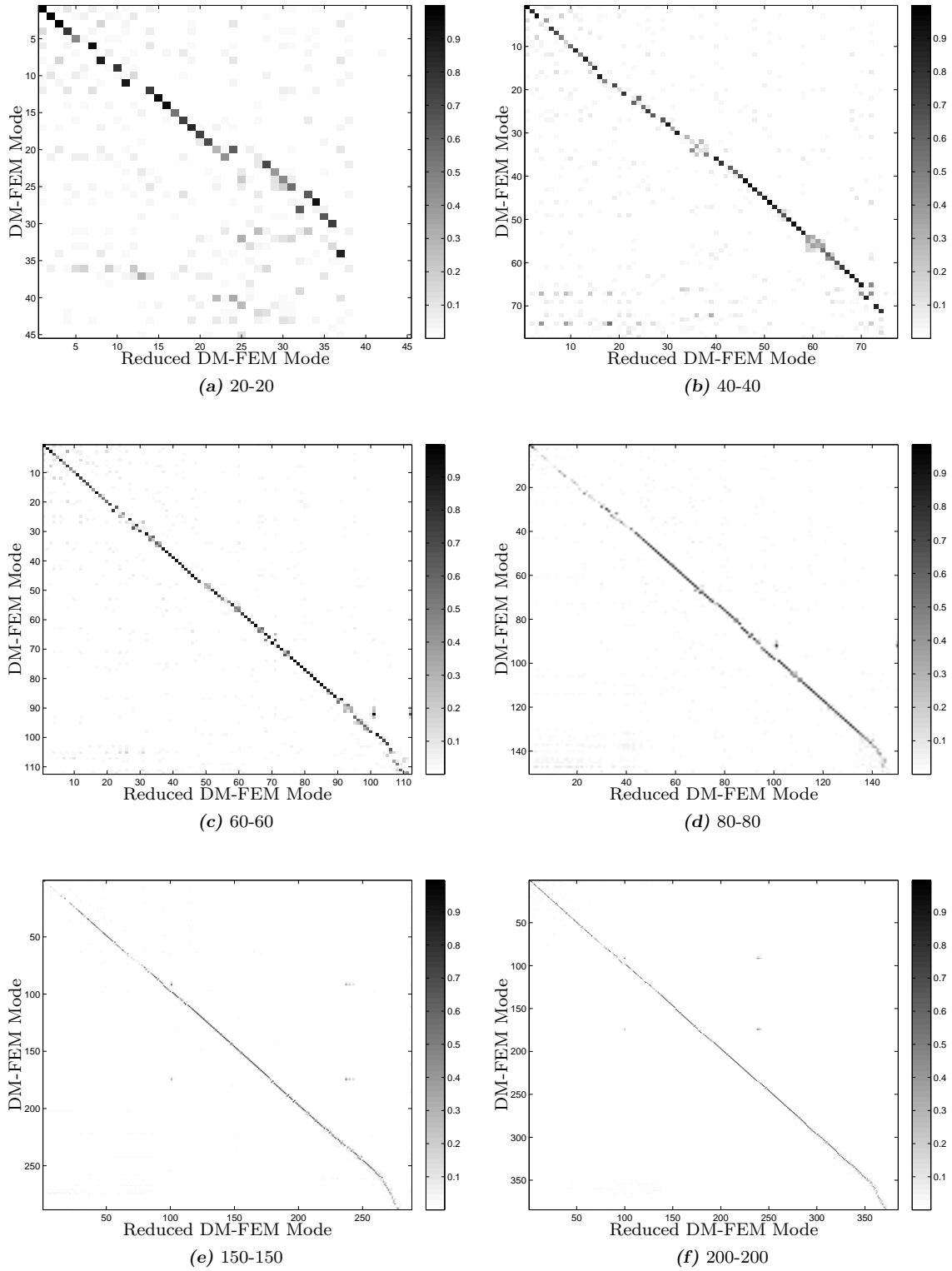


Figure 6: MAC criterion for each modes (method *Fre-Fix-2*: truncations: a:20-20, b:40-40, c:60-60, d:80-80, e:150-150, f:200-200)

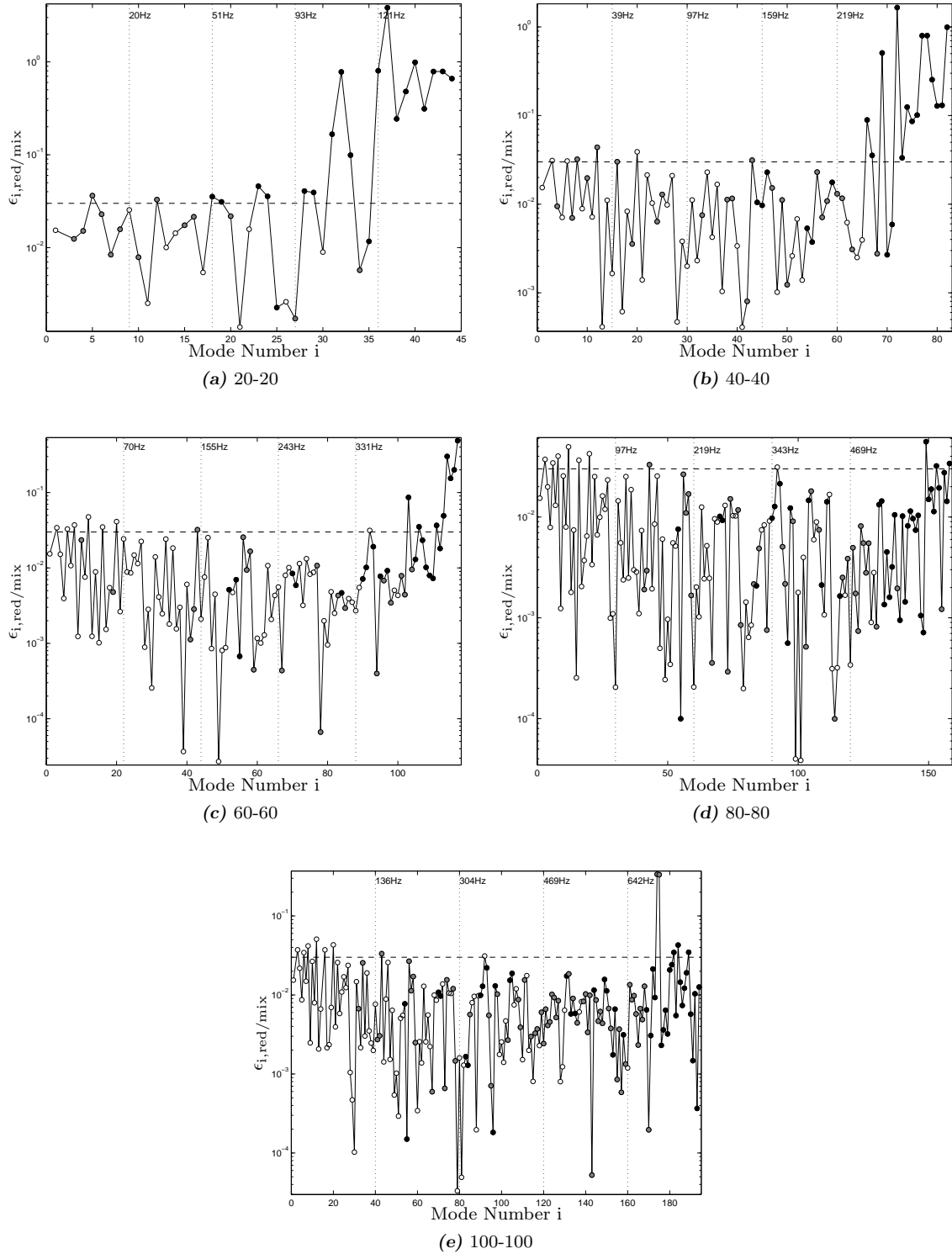


Figure 7: Relative error on the eigenfrequencies $\epsilon_{i,red}/mix$ in function of the mode i and insight of the MAC criterion for each modes (method Fre-Fre-1: truncations: a:20-20, b:40-40, c:60-60, d:80-80, e:100-100)

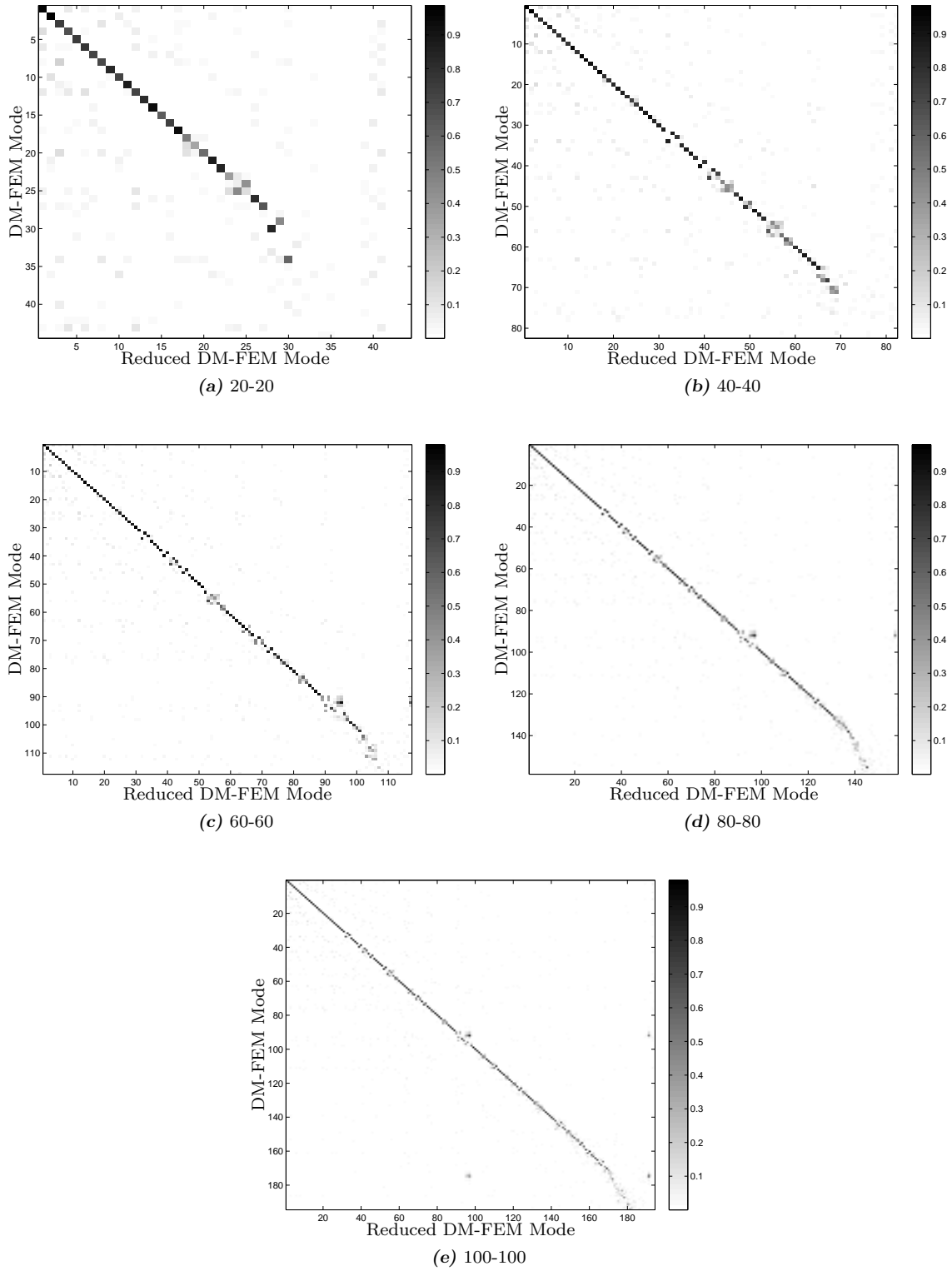
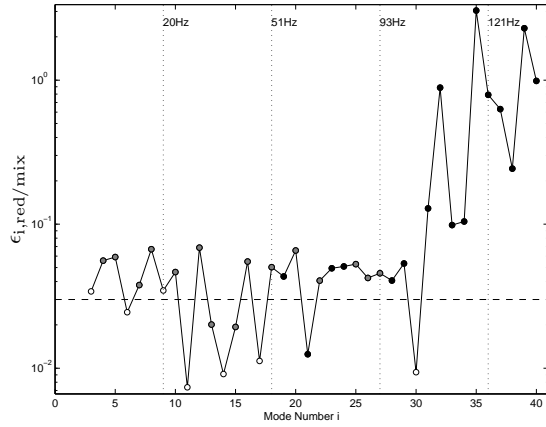
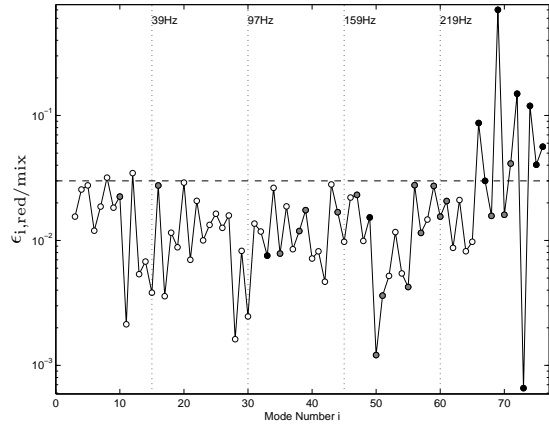


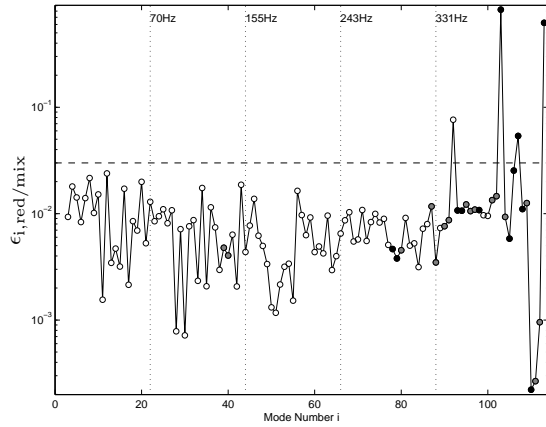
Figure 8: MAC criterion for each modes (method Fre-Fre-1: truncations: a:20-20, b:40-40, c:60-60, d:80-80, e:100-100)



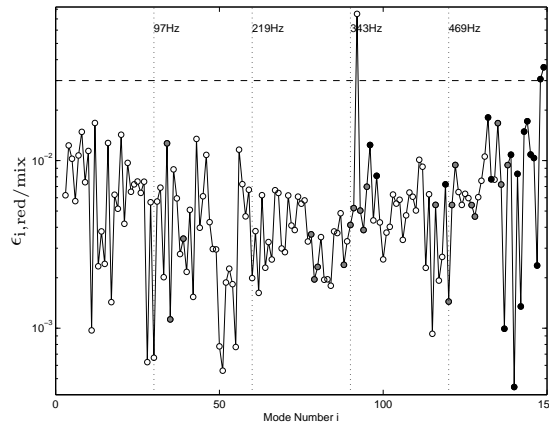
(a) 20-20



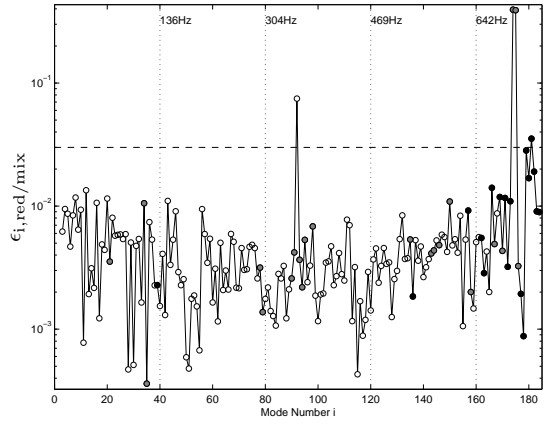
(b) 40-40



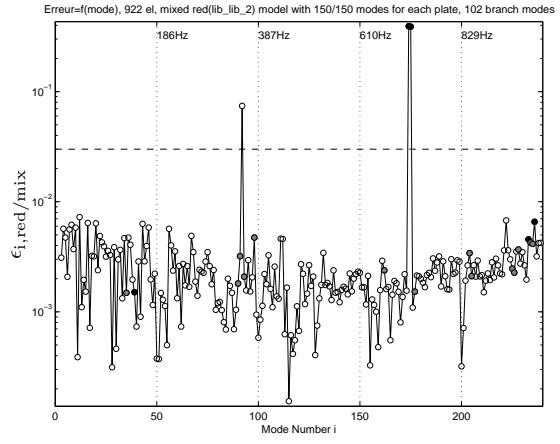
(c) 60-60



(d) 80-80



(e) 100-100



(f) 150-150

Figure 9: Relative error on the eigenfrequencies $\epsilon_{i,\text{red}/\text{mix}}$ in function of the mode i and insight of the MAC criterion for each modes (method Fre-Fre-2: truncations: a:20-20, b:40-40, c:60-60, d:80-80, e:100-100, f:150-150)

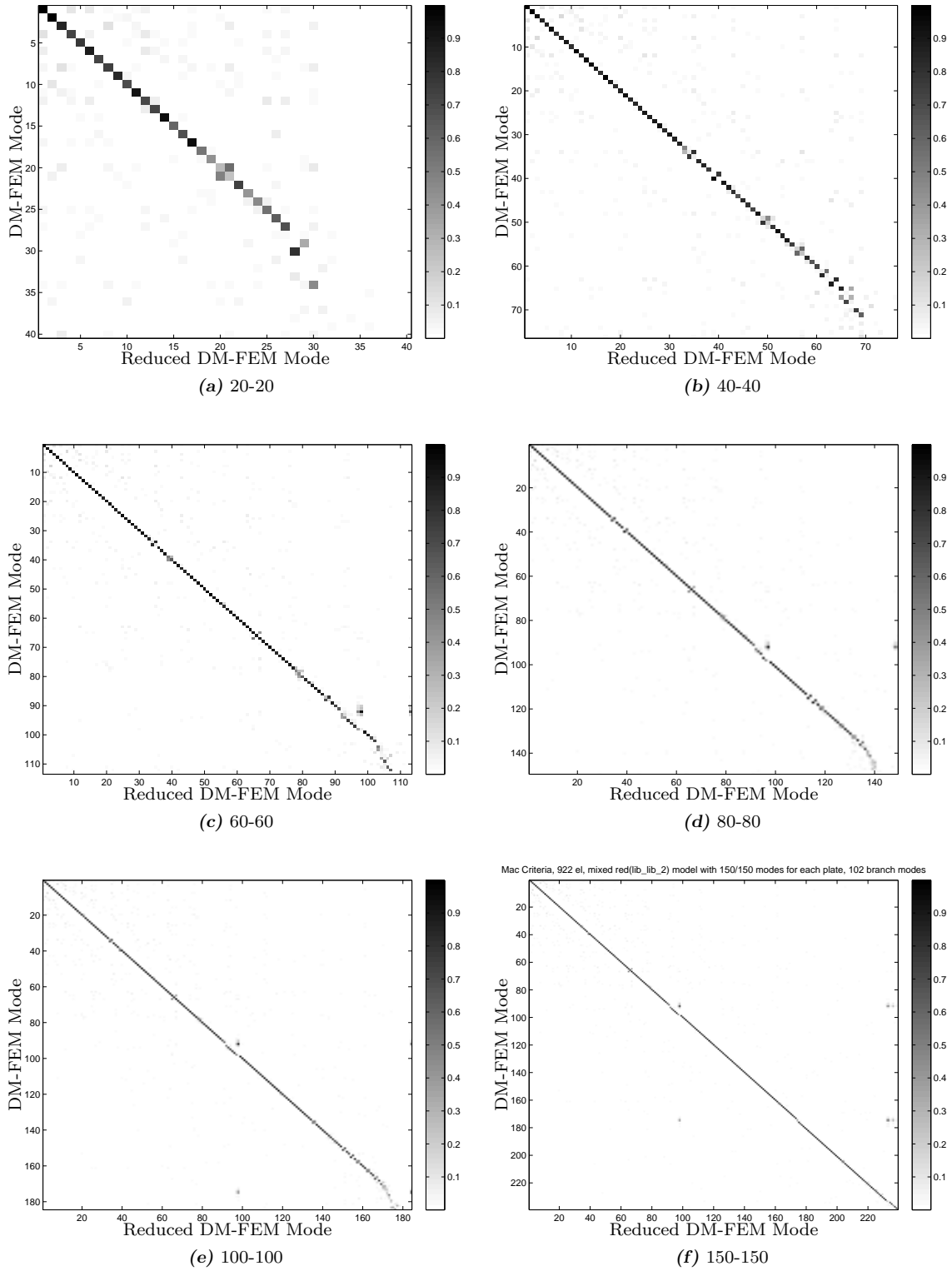


Figure 10: MAC criterion for each modes (method Fre-Fre-2: truncations: a:20-20, b:40-40, c:60-60, d:80-80, e:100-100, f:150-150)

The Fre-Fre-2 method shows good results. In fact, whereas there is no differences between the results of Fix-Fix-1 and Fix-Fix-2 methods, we note some differences between Fre-Fre-1 and Fre-Fre-2.

For the biggest truncations (20-20, 40-40, 60-60, 80-80), the limit frequency is the same as for the Fre-Fre-1 method. Nevertheless, when the truncation is small (100-100, 150-150), the converged frequency band is better with the Fre-Fre-2 method.

The biggest improvement comparing to the Fre-Fre-1 method concerns the density of "singular modes" which is much better as long as the truncation is not too big. For example, the truncations 60-60, 80-80 100-100, 150-150 show a density less than 16%, which gives us a much better convergence on the frequency band for this method. Nevertheless, it is important to notice than the density of singular modes can be high if the number of modes kept in the truncation is too small (example: 20 – 20 and 40 – 40 truncations with respectively 78% and 28%).

4.5. Convergence study: truncation of the branch modes

This section deals with the results obtained when truncating the branch modes. The idea is to keep the results from the last section and truncate the branch modes in addition to the internal truncation, to reduce the junction, and check the signal degradation. The example remains the same, and the checking method with both relative error and MAC criterion as well. We want to compare the limit frequency and the density of the "singular modes" with the previous truncations, in function of the number of branch modes remaining. The Fre-Fix-2 and Fre-Fre-1 methods having insufficient results, the use of branch modes truncation with it will not be discuss in this section. Nevertheless, the Fix-Fix-1or2 and Fre-Fre-2 methods are treated.

The first results show that the limit frequency basically remains the same with any branch modes truncation. The most relevant point to focus on is the density of "singular modes" that varies in function of the number of branch modes remaining in the reduced model. The more the density of "singular modes" is high, the more degraded the dynamic response is, and the less relevant the reduction is, as expected.

4.5.1. Fix-Fix-1 or Fix-Fix-2 method

The table 5 and figure 11 show the evolution of the "singular modes" density in function of the truncation of the branch modes, for the Fix-Fix-1or2 method, for each of the six different truncations (of internal modes) implemented for this method (see table 5).

An overview is made by figure 11. It appears that, for each different truncation, a certain number of branch modes is necessary to keep the response as good as it was with no truncation. Using less branch modes highly degrades the response, whereas using more doesn't improve the signal. Nevertheless, the number of branch modes needed varies in function of the initial truncation of internal modes. The higher the truncation of internal modes is, the higher the truncation of branch modes can be.

An explanation of this phenomenon can found in table 5 in which is listed, the frequency of the last truncated branch modes, that is to say the lowest frequency of the branch modes that is not taken into consideration in the reduced model. If we compare the converged frequency band

of the reduced model with no branch mode truncation (example: $0 - 149Hz$ for the 20-20 reduction) and the value of the lowest frequency truncated in the branch modes (example: $203Hz$ for 5 branch modes remaining and $90Hz$ for 4 branch modes remaining), we can be lead to a conclusion. Indeed, when a branch mode whose frequency is in the frequency band "supposedly converged", the truncation of this mode will degrades the response (example: 20-20-4 getting 33% of "singular modes"). On the other hand, when we keep all the modes whose frequencies are in the frequency band converged with no branch modes truncation, we keep a low degradation of the response (low density of "singular modes"). In the table 5, those two domains are splitted with a simple line. Furthermore, it appears that when the last truncated branch mode is at least twice bigger than the highest frequency of the band, the response of the reduced structure is the same as with the whole set of branch modes, which means it doesn't deteriorate the dynamic behavior of the reduced structure.

The results of this part show that, for the Fix-Fix-1 or Fix-Fix-2 method, we can easily decrease the number of junction DOFs and keep a great representation of the structure, as long as we stay in the good frequency range.

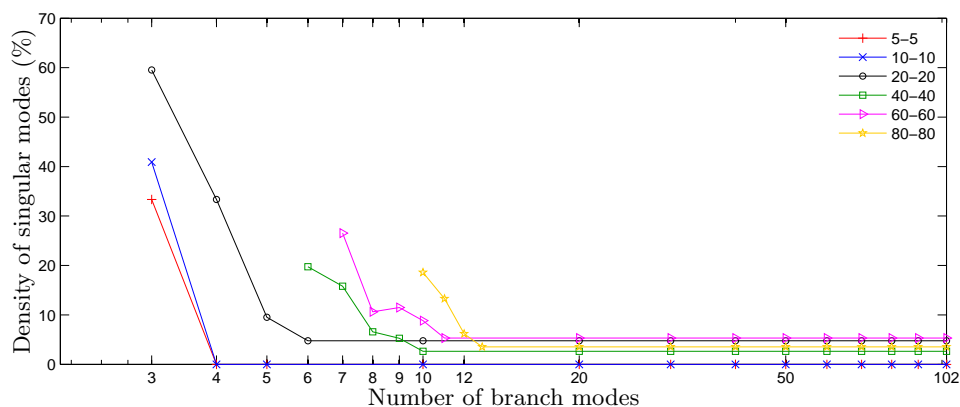


Figure 11: Density of "singular modes" in function of the branch modes truncation for the Fix-Fix-1or2 method

4.5.2. Fre-Fre-2 method

The figure 12 shows the evolution of the "singular modes" density in function of the truncation of the branch modes, for the Fre-Fre-2 method, for each of the five different truncations (of internal modes) implemented for this method (see table 5).

The results doesn't seem very relevant as the amount of "singular modes" increases even with small truncations, and doesn't seem to follow a particular rule. It appears that, when keeping at least 90 modes out of 102 branch modes, it doesn't alter the dynamic response, but as soon as the truncation is bigger, the density of singular modes increases. Between 30 and 80 branch modes, the number of "singular modes" seems to be steady, and seems to decrease a little bit between 30 and 15 branch modes. Then when truncating even more, this method follows the same rule as the Fix-Fix-1or2 method as the response is more and more deteriorate. All in all, the truncation of branch modes doesn't seem very efficient with the Fre-Fre-2 method as there is no particular rule to follow and the truncations allow is very small. It sounds safer to use the Fre-Fre-2 method without

Table 6: Results for different truncations of branch modes, using the Fix-Fix-1or2 method

Truncation name	Branch modes	Limit mode	Limit freq (Hz)	Singular modes nb	Singular modes %	Lowest frequency truncated among the branch modes	DOFs method 1	DOFs method 2
Primal non-reduced method							2958	
Mixed non-reduced method							11256	
5-5-102	102	12	33	0	0%	FULL	112	122
5-5-4	4	12	33	0	0%	90	14	24
5-5-3	3	12	33	4	33%	14	13	23
10-10-102	102	22	70	0	0%	FULL	122	142
10-10-5	5	22	70	0	0%	203	25	45
10-10-4	4	22	70	2	9%	90	24	44
10-10-3	3	22	70	9	41%	14	23	43
20-20-102	102	42	149	2	4.8%	FULL	142	182
20-20-6	6	42	149	2	4.8%	226	46	86
20-20-5	5	42	149	4	6.5%	203	45	85
20-20-4	4	42	149	14	33%	90	44	84
20-20-3	3	42	149	25	59%	13	43	83
40-40-102	102	76	290	2	2.6%	FULL	182	262
40-40-10	10	76	290	2	2.6%	579	90	170
40-40-9	9	76	290	4	5.2%	502	89	169
40-40-8	8	76	290	5	6.5%	430	88	168
40-40-7	7	76	290	12	16%	287	87	167
40-40-6	6	76	290	15	20%	227	86	166
60-60-102	102	113	447	6	5.3%	FULL	222	342
60-60-11	11	113	447	6	5.3%	914	131	251
60-60-10	10	113	447	10	9%	579	130	250
60-60-9	9	113	447	13	11.5%	502	129	249
60-60-8	8	113	447	12	10.6%	430	128	248
60-60-7	7	113	447	30	26.5%	287	127	247
80-80-102	102	147	580	4	2.7%	FULL	262	422
80-80-13	13	147	580	4	2.7%	1102	173	333
80-80-12	12	147	580	7	4.8%	963	172	332
80-80-11	11	147	580	15	10.7%	914	171	331
80-80-10	10	147	580	21	14.3%	430	170	330

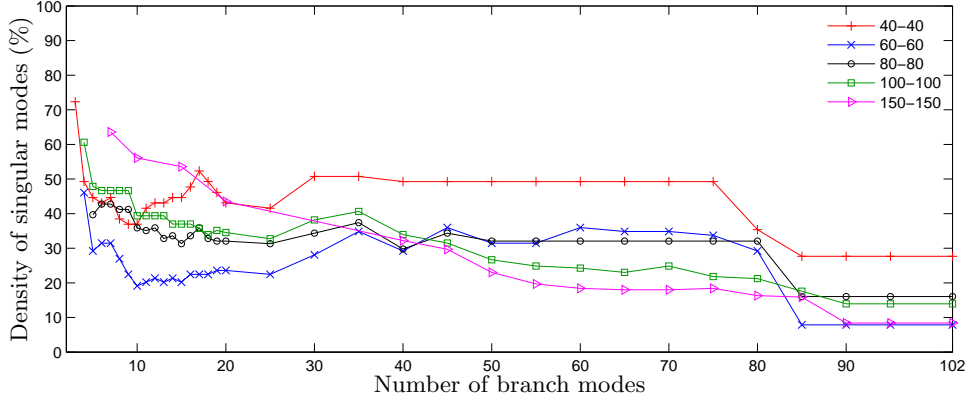


Figure 12: Density of "singular modes" in function of the branch modes truncation for the Fre-Fre-2 method

the branch mode truncation.

5. CONCLUSIONS

The purpose of this paper is to set various reduction methods to decrease the numerical size of a DM-FEM. Indeed, mixed model discretize both displacement and stress fields and therefore use big size matrices to compute the dynamic response of a complex structure. The first principle of those methods is to split the global structure into few substructures and to reduce each of them separately. The second principle and the originality of those method is to separate the projection of the two different fields and to use eigenmodes taken from the primal structure to build a new reduced basis for the DM-FEM. The differentiation between the two fields allows to choose different types of reduction depending on the field and therefore to imagine a whole set of combinations.

In this paper we implement five different reduction methods with different results, and for each method we also have the possibility to reduce the junction, using "branch modes". The primal method we adapt for each fields are "fixed mode" methods (boundary between the substructures assumed fixed) or "free mode" methods (boundary assumed free). The Fix-Fix-1 and Fix-Fix-2 methods use both "fixed mode" methods for the displacement and stress fields, and the "1" extension means reduced parameters for the two fields are gathered, whereas the "2" extension means they are separated. The Fre-Fix-2 method use "free modes" for the displacements and "fixed modes" for the stresses. The Fre-Fre-1 and Fre-Fre-2 methods use both "free modes" for both fields with the extension featuring the same as Fix-Fix-1 and Fix-Fix-2 methods.

The table 5 summarizes the results we obtained through the different reductions methods (without the "branch modes" truncation). The Fix-Fix-1 and Fix-Fix2 methods are the most efficient with our examples. They both give the exact same result, and permit to significantly decrease the number of DOFs and still keep a good representation. As an example, when using the 40-40 truncation (that-is-to-say 40 displacement modes and 40 stress modes), the reduced DM-FEM still have a good representation for the 76 first modes and reduced the size from 11256 DOFs to 262. The other truncations computed with those methods give good results as well. The Fre-Fre-2

method is the second most efficient methods. The differences with the previous methods, for the same truncations, is the converged frequency band that is a bit smaller, but also an amount of "singular modes" that is slightly higher. Furthermore, the results diverge with high truncations (10-10, 20-20, 40-40), so the method is only efficient for 60-60 modes remaining and above.

Although, the Fix-Fix-1 and Fix-Fix-2 methods give the exact same results, the Fre-Fre-1 method has different results from the Fre-Fre-2 method. The major difference lays in the bigger density of "singular modes". Indeed, even though the limit frequency is as high as the Fre-Fre-2 method, the amount of modes not well enough defined in terms of form and frequency is too high to consider this method as relevant.

Lastly, the Fre-Fix-2 method that mixes both "free" and "fixed modes" methods lead to poor results with too many singular modes all over the frequency band observed.

In the end, we reduced the size of the junction, with the use of branch modes that are supposed to feature the behavior of the junction and the behavior of the substructures associated. We only study the Fix-Fix-1or2 and Fre-Fre-2 methods in this section. The results are summarized in table . It appears that the use of branch modes is highly efficient for the Fix-Fix-1or2 method for all the truncations of internal modes we implemented, as we can truncate all the branch modes whose frequencies are at least twice bigger than the highest frequency represented by the method. It allows us to reduce the size of the junction from 102 DOFs to around 10 DOFs for the truncations we implemented. Nevertheless, the use of branch modes with the Fre-Fre-2 method was not relevant.

So as to conclude, the use of the Fix-Fix-1 with a truncation of branch modes leads to really powerful results as we can decrease the number of DOFs of the DM-FEM from 11256 to respectively 14, 25, 46, 90, 131 and 173 DOFs, and keep a good representation of respectively the 12, 22, 42, 76, 113 and 147 first modes, and keep the advantages of the mixed formulation.

ACKNOWLEDGEMENT

The first author gratefully acknowledges the French Education Ministry which supports this research.

BIBLIOGRAPHY

- [1] J.H. Argyris. Continua and discontinua. Proc. Conf. Matrix Meth. Struct. mech., pages 11–190, 1965.
- [2] D.N. Arnold, F. Brezzi, and J.Jr. Douglas. Peers: A new mixed finite element for plane elasticity. Japan Journal of Applied Mathematics, 1984.
- [3] D.N. Arnold and R.S. Falk. A new mixed formulation for elasticity. Numerische Mathematik, 53(1-2):13–30, 1988.
- [4] D.N. Arnold and R. Winther. Mixed finite element for elasticity in the stress-displacement formulation. Contemporary Mathematics, 2003.
- [5] R. Ayad, G. Dhatt, and J.L. Batoz. A new hybrid variational approach for reissner-mindlin plates. the misp model. International Journal for Numerical Methods in Engineering, 42:1149–1179, 1998.

- [6] I. Babuska. The finite element method with lagrangian multipliers. Numerische Mathematik, 20(3):179–192, 1973.
- [7] E. Balmes. Use of generalized interface degrees of freedom in component mode synthesis. Proceeding of IMAC, pages 204–210, 1996.
- [8] K.J. Bathe and E.N. Dvorkin. Short communication a four-node plate bending element based on mindlin/reissner plate theory and a mixed interpolation. International Journal For Numerical Methods in Engineering, 21:367–383, 1985.
- [9] K.J. Bathe and E.N. Dvorkin. A formulation of general shell elements - the use of mixed interpolation of tensorial components. International Journal For Numerical Methods In Engineering, 22:697–722, 1986.
- [10] A. Benjeddou. Advances in piezoelectric finite element modeling of adaptative structural elements: a survey. Computers and Structures, 76:347–363, 2000.
- [11] A. Benjeddou and O. Andrianarison. A thermopiezoelectric mixed variational theorem for smart, multilayered composites. Computers and Structures, 83:1266–1276, 2005.
- [12] S. Besset and L. Jézéquel. Dynamic sub-structuring based on a double modal analysis. Journal of Vibration and acoustics, 130(1):011008, 2008.
- [13] K.U. Bletzinger, M. Bischoff, and E. Ramm. A unified approach for shear-locking-free triangular and rectangular shell finite element. Computers and Structures, 75:321–334, 2000.
- [14] F. Brezzi. On the existence, uniqueness and approximation of saddle-point problems arising from lagrangian multipliers. Revue Francaise d’Automatique, informatique, rechefeceh opérationnelle, analyse numérique, 8(2):129–151, 1974.
- [15] D. Brizard, L. Jézéquel, S. Besset, and B. Troclet. Determinantal method for locally modified structures. application to the vibration damping of a space launcher. Computational Mechanics, 20:631–644, 2012.
- [16] J. Bron and G. Dhatt. Mixed quadrilateral elements for bending. AIAA Journal, 10:1359–1361, 1972.
- [17] E. Carrera. Cz requirements - models for the two-dimensional analysis of multilayered structures. Composite and Structures, 37:373–383, 1997.
- [18] E. Carrera. An improved reissner-mindlin-type model for the electromechanical analysis of multilayered plates including piezo-layers. Journal of Intelligent Materials Systems and Structures, 8:232–248, 1997.
- [19] E. Carrera. Evaluation of layerwise mixed theories for laminated plate analysis. AIAA Journal, 36:830–839, 1998.
- [20] E. Carrera. An assesment of mixed and classical theories for the thermal stress analysis of orthotropic multilayered plates. Journal of Thermal Stresses, 23:797–831, 2000.
- [21] E. Carrera. Developments, ideas, and evaluations based upon reissner’s mixed variational theorem in the modeling of multilayered plates and shells. Applied Mechanics Reviews, 54:301–329, 2001.

- [22] E. Carrera and M. Boscolo. Classical and mixed finite element for static and dynamic analysis of piezoelectric plates. International Journal For Numerical Methods In Engineering, 70:1135–1181, 2007.
- [23] E. Carrera and L. Demasi. Classical and advanced multilayered plate elements based upon pvd and rmvt. part 1: Derivation of finite element matrices. International Journal for Numerical Methods in Engineering, 55:191–231, 2002.
- [24] E. Carrera and L. Demasi. Classical and advanced multilayered plate elements based upon pvd and rmvt. part 2: Numerical implementation. International Journal for Numerical Methods in Engineering, 55:253–291, 2002.
- [25] A. Chatterjee and A.V. Setlur. A mixed finite element formulation for plate problems. International Journal For Numerical Methods In Engineering, 4:67–84, 1972.
- [26] M. Cho and R. Parmerter. Efficient higher order composite plate theory for general lamination configurations. AIAA Journal, 31(7):1299–1306, 1993.
- [27] R.W. Clough and J.I. Tocher. Finite element stiffness matrix for the analysis for plate bending. Proc. Conf. Matrix Meth. Struct. mech., pages 515–546, 1965.
- [28] R.R. Craig. Coupling of substructures for dynamic analysis: an overview. AIAA Journal, 1573, 2000.
- [29] R.R. Craig and M.C.C. Bampton. Coupling of substructures for dynamic analysis. AIAA Journal, 6(7):1313–1319, 1968.
- [30] S. de Miranda and F. Ubertini. A simple hybrid stress element for shear deformable plates. International Journal for Numerical Methods in Engineering, 65:808–833, 2006.
- [31] M. Duan, Y. Miyamoto, S. Iwasaki, and H. Deto. Numerical implementation of hybrid-mixed finite element model for reissner-mindlin plates. Finite Element in Analysis and Design, 33:167–185, 1999.
- [32] N. Fantuzzi and F. Tornabene. Strong formulation finite element method for arbitrarily shaped laminated plates - part 1. theoretical analysis. Advances in Aircraft and Spacecraft Science, 1:125–143, 2014.
- [33] N. Fantuzzi and F. Tornabene. Strong formulation finite element method for arbitrarily shaped laminated plates - part 2. numerical analysis. Advances in Aircraft and Spacecraft Science, 1:145–175, 2014.
- [34] N. Fantuzzi, F. Tornabene, E. Viola, and A.J.M. Ferreira. A strong formulation finite element method (sfem) based on rbf and gdq techniques for the static and dynamic analyses of laminated plates of arbitrary shape. Meccanica, 49:2503–2542, 2014.
- [35] B. Fraeijs de Veubeke. Displacement and equilibrium models in the finite element method, chapter 9. John Wiley & Sons, 1965.
- [36] B. Fraeijs de Veubeke and G. Sander. An equilibrium model for plate bending. International Journal of Solids and Structures, 4:447–768, 1968.
- [37] P. Garambois, S. Besset, and L. Jézéquel. Modal synthesis applied to a reissner mixed plate finite element dynamic model. Proceedings of the 9th International Conference on Structural Dynamics, EUROLYN 2014, 2014.

- [38] R. Garcia Lage, C.M. Mota Soares, C.A. Mota Soares, and J.N. Reddy. Analysis of adaptative plate structures by mixed layerwise finite elements. Composite Structures, 66:269–276, 2004.
- [39] R. Garcia Lage, C.M. Mota Soares, C.A. Mota Soares, and J.N. Reddy. Modelling of piezo-lamited plates using layerwise mixed elements. Computers and Structures, 82:1849–1863, 2004.
- [40] M. Gellert and M.E. Laursen. Formulation and convergence of a mixed finite element method applied to elastic arches of arbitrary geometry and loading. Computer Methods In Applied Mechanics and Engineering, 7:285–302, 1976.
- [41] E. Hellinger. Die allgemeinen ansatze der mechanik der kontinua. Encyklopadie der mathematischen Wissenschaften, 4, 1914.
- [42] L.R. Herrmann. A bending analysis for plates. Proceeding of the conference on matrix methods in structural mechanics, A.F.F.D.L-TR-66-88, pages 577–604, 1965.
- [43] L.R. Herrmann. Finite element bending analysis. Journal of the Engineering Mechanics Division, A.S.C.E EM5, 93:13–26, 1967.
- [44] T.J.R. Hughes, M. Cohen, and M. Haron. Reduced and selective integration techniques in the finite element analysis of plates. Nuclear Engineering and Design, 46:203–222, 1978.
- [45] L. Jézéquel and H.D. Setio. Component modal synthesis methods based on hybrid models, part 1: Theory of hybrid models and modal truncation methods. Journal of Applied mechanics, 61:100–108, 1994.
- [46] F. Koschnick, M. Bischoff, N. Camprubì, and K.U. Bletzinger. The discrete strain gap method and membrane locking. Computer Methods in Applied Mechanics and Engineering, 194:2444–2463, 2005.
- [47] S.W. Lee and J.J. Rhiu. A new efficient approach to the formulation of mixed finite element model for structural analysis. International Journal For Numerical Methods In Engineering, 21:1629–1641, 1986.
- [48] K.H. Lo, R.M. Christensen, and M. Wu. A high-order theory of plate deformation—part 2: Laminated plates. Journal of Applied Mechanics, 44:669–676, 1977.
- [49] A.E.H. Love. On the small free vibrations and deformations of elastic shells. Philosophical Transactions of the Royal Society of London, 17:491–549, 1888.
- [50] R.H. MacNeal. A hybrid method of component mode synthesis. Computers and Structures, 1:581–601, 1971.
- [51] R.D. Mindlin. Influence of rotatory inertia and shear on flexual motions of isotropic, elastic plates. Journal of Applied Mechanics, 18:31–38, 1951.
- [52] H. Nguyen-Xuan, G.R. Liu, C. Thai-Hoang, and T. Nguyen-Thoi. An edge-based smoothed finite element method (es-fem) with stabilized discrete shear gap technique for analysis of reissner-mindlin plates. Computational Method Applied for Mechanical Engineering, 199:471–489, 2010.
- [53] M.H. Omurtag and F. Kadioglu. Free vibration analysis of orthotropic plates resting on paster-nak foundation by mixed finite element formulation. Computers and Structures, 67:253–265, 1998.

- [54] T.H.H. Pian, D.P. Chen, and D. Kang. A new formulation of hybrid/mixed finite element. Computers & Structures, 16:81–87, 1983.
- [55] T.H.H. Pian and P. Tong. Finite element methods in continuum mechanics. Advances in Applied Mechanics, 12:1–58, 1972.
- [56] G. Prange. Die variations- und minimalprinzip der statik der baukonstruktion. Habilitationsschrift, Technische Hochschule Hannover, 1916.
- [57] J.N. Reddy. A generalization of two-dimensional theories of laminated composite plates. Communications in Applied Numerical Methods, 3:173–180, 1987.
- [58] J.N. Reddy. Theory and Analysis of Elastic Plates and Shells. 2007.
- [59] E. Reissner. The effect of transverse shear deformation on the bending of elastic plates. Journal of Applied Mechanics, 12:69–76, 1945.
- [60] E. Reissner. On a variational theorem in elasticity. Journal of Mathematics and Physics, 29:90–95, 1950.
- [61] E. Reissner. On a certain mixed variational theorem and a proposed application. International Journal For Numerical Methods In Engineering, 20(7):1366–1368, 1984.
- [62] E. Reissner. On a mixed variational theorem and on shear deformable plate theory. International Journal For Numerical Methods In Engineering, 23(2):193–198, 1986.
- [63] A.F. Saleeb and T.Y. Chang. On the hybrid-mixed formulation of c0 curved beams. Computer Method in Applied Mechanics and Engineering, 60:95–121, 1987.
- [64] N. Srinivas. A refined analysis of composite laminates. Journal of Sound and Vibration, 30(4):495–507, 1973.
- [65] H. Stolarski and T. Belytschko. Shear and membrane locking in curved c0 elements. Computer methods in applied mechanics and engineering, 41:279–296, 1983.
- [66] H. Stolarski and T. Belytschko. On the equivalence of mode decomposition and mixed finite element based on the hellinger-reissner principle. part 1: Theory. Computers Methods in Applied Mechanics and Engineering, 58:249–263, 1986.
- [67] H. Stolarski and T. Belytschko. On the equivalence of mode decomposition and mixed finite element based on the hellinger-reissner principle. part 2: Application. Computers Methods in Applied Mechanics and Engineering, 58:265–284, 1986.
- [68] P. Tong and T.H.H. Pian. A variational principle and the convergence of a finite element method based on assumed stress distribution. International Journal of Solids and Structures, 5:463–472, 1969.
- [69] F. Tornabene, N. Fantuzzi, E. Viola, and R.C. Batra. Stress and strains recovery for functionally graded free-form and doubly-curved sandwich shells using higher-order equivalent single layer theory. Composite and Structures, 119:67–89, 2015.
- [70] D.M. Tran. Component mode synthesis methods using interface modes. application to structures with cyclic symmetry. Computers and Structures, 79:209–222, 2001.
- [71] K. Washizu. Variational methods in elasticity and plasticity, 2nd edition. Pergamon Press, 1975.

- [72] P. Wriggers and C. Carstensen. Mixed Finite Element Technologies. Applied Mathematics/Computational Methods of Engineering, 2009.
- [73] F. Wu, G.R. Liu, G.Y. Li, A.G. Cheng, and Z.C. He. A new hybrid-smoothed fem for static and free vibration analyses of reissner-mindlin plates. Computational Mechanics, 2014.
- [74] P.C. Yang, C.H. Norris, and Y. Stavsky. Elastic wave propagation in heterogeneous plates. International Journal of Solids and Structures, 2:665–684, 1966.
- [75] O.C. Zienkiewicz and Y.K. Cheung. The finite element method in structural and continuum mechanics. McGraw-Hill, 1967.